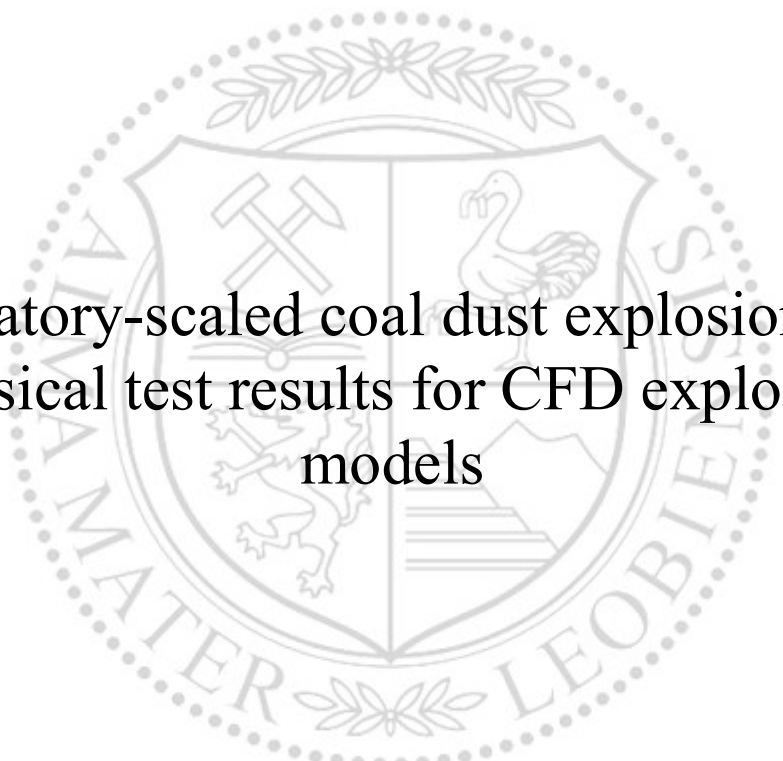




Chair of Mining Engineering and Mineral Economics

Master's Thesis



Laboratory-scaled coal dust explosions and  
physical test results for CFD explosion  
models

Patrick Maier, BSc

March 2020



## EIDESSTATTLICHE ERKLÄRUNG

Ich erkläre an Eides statt, dass ich diese Arbeit selbständig verfasst, andere als die angegebenen Quellen und Hilfsmittel nicht benutzt, und mich auch sonst keiner unerlaubten Hilfsmittel bedient habe.

Ich erkläre, dass ich die Richtlinien des Senats der Montanuniversität Leoben zu "Gute wissenschaftliche Praxis" gelesen, verstanden und befolgt habe.

Weiters erkläre ich, dass die elektronische und gedruckte Version der eingereichten wissenschaftlichen Abschlussarbeit formal und inhaltlich identisch sind.

Datum 19.02.2020

Unterschrift Verfasser/in  
Patrick, Maier

---

## Danksagung / Acknowledgements

---

Als erstes möchte ich mich bei meinen zwei Betreuern: Dr. Philipp Hartlieb, der es mir ermöglichte, diese Arbeit im Ausland auszuführen und Dr. Jürgen F. Brune (CSM) für seine Hilfe und Anleitung bei der Umsetzung dieses Projekts, sowie der Verwirklichung meines erfolgreichen Auslandsaufenthaltes in Golden, CO. Ein besonderer Dank gilt Herrn Dr. Gregory E. Bogin, Jr. Er hatte immer Zeit für Fragen und half mir bei der Umsetzung meiner Versuche. Weiters bedanke ich bei Dr. Richard Gilmore für die hilfreichen Diskussionen. Auch gilt mein Dank an Yunfei Zhu, der mich jederzeit unterstützt hat.

Mein aufrichtiger Dank gilt meinen Eltern, Uta und Ewald, und meiner Schwester Verena für ihre Unterstützung und dass sie nie an meinen Entscheidungen gezweifelt haben. Mein zusätzlicher Dank gilt meinem all meinen Freunden zuhause und in Amerika, die mir bei meinen Problemen zugehört haben und mir immer positiv zugeredet haben.

I would like to thank my two advisors: Dr. Philipp Hartlieb, who enabled me to do that Master's thesis abroad, and Dr. Jürgen F. Brune (CSM) for his assistance and guidance in this project, as well as in my successful abroad visit at CSM in Golden, CO. Thank you in particular to Dr Gregory E. Bogin, Jr. He always had time to answer my questions and helped me conducting my experiments. I would also like to thank Dr. Richard Gilmore for the helpful discussions. I would also like to thank Yunfei Zhu who has supported me.

I thank my parents Uta and Ewald, and my sister Verena, sincerely for their support, and for never doubting my choices. I thank my friends in my home country and in America for listening to my difficulties and always talking to me positively.

---

## Zusammenfassung

---

Explosionen von Kohlenstaub im untertägigen Kohlebergwerken können katastrophale Folgen mit vielen Todesopfern und schweren Sachschäden verursachen. Die Explosion im Untertagebergwerk Upper Big Branch in West Virginia, USA, im Jahr 2010 hat 29 Todesopfer gefordert. Diese Katastrophe hat gezeigt, dass Explosionen von Kohlestaub in untertägige Kohlebergbau immer noch vorkommen können, wenn die Präventivmaßnahmen unzureichend sind. Seit der Schließung des Versuchsbergwerks NIOSH Lake Lynn Laboratory, in dem die Ausbreitung von Kohlenstaubexplosionen untersucht wurde, gibt es in den Vereinigten Staaten keine großmaßstäblichen physikalischen Testeinrichtungen für die Prüfung der Verhinderung von Kohlenstaubexplosionen mehr. In Polen (Versuchsbergwerk Barbara) sind Versuche in vollem Umfang noch möglich, doch diese sind mit hohen Reise- und Durchführungskosten von Experimenten verbunden. Physikalische Tests im Maßstab 1:5 bis 1:50 in Kombination mit numerischen Modellen der Computational Fluid Dynamics (CFD) helfen Wissenschaftlern, die Komplexität der mehrphasigen chemischen Reaktionen, die thermodynamischen Mechanismen und die turbulente Strömungsdynamik besser zu verstehen. Durch maßstäbliche Tests mit CFD werden realistische Modelle zur Untersuchung der Gefahren und der Vermeidung von Kohlenstaubexplosionen in untertägigen Kohlebergbaue erstellt.

Das Ziel dieser Arbeit ist es, skalierte Methan- und Kohlenstaubexplosionen zur Validierung von CFD-Modellen zu untersuchen. Die Tests wurden in einem horizontalen, zylindrischen Stahlreaktor mit 63 mm Durchmesser und 1.5 m Länge im Maßstab von ca. 1:30 durchgeführt. Das Volumen des Reaktors betrug 4,8 L. Eine Reihe von Tests wurde mit unterschiedlichen Kohlestaubkonzentrationen durchgeführt. Der Staub wurde in den ersten Versuchen von einer Metallplatte im Inneren des Reaktors aufgewirbelt. Sensoren wurden eingesetzt, um die Flammengeschwindigkeit und den Druck an verschiedenen Punkten entlang des Reaktors zu messen. Die ersten Ergebnisse zeigten, dass die von der Flamme erzeugte Wärme zu gering war, um die flüchtigen Bestandteile der Kohlenstaubpartikel freizusetzen. Der Kohlenstaub absorbiert die Wärme und verringert die Geschwindigkeit der Flamme, weil die Kohlenstaubpartikel der Flamme nur für kurze Zeit ausgesetzt waren.

In der zweiten Testreihe wurde aufgewirbelter Kohlenstaub benutzt, unter der Hypothese durchgeführt, dass die brennbare Staubwolke die Flammgeschwindigkeit in dem Methan-Luft-Gemisch erhöht. Der Staub wurde kurz vor der Entzündung des Methan-Luft-Gemisches über ein Düsenrohr in den Reaktor eingeblasen.

Ein weiteres Ziel dieser Arbeit war es, einen Reaktor mit einer längeren Reaktionszone für die Kohlestaubpartikel zu entwerfen und zu konstruieren. Der zweite Reaktor ist 1,5 m lang und hat Seitenwänden aus Plexiglas. Dies ermöglicht eine visuelle Untersuchung der Mitnahme von Kohlenstaubpartikeln und der Wechselwirkung mit der Methanflamme. Mit diesem Reaktor werden weitere Forschungsarbeiten durchgeführt, um die Dynamik der Staubbewegung und der Verbrennung der Kohlepartikel zu verstehen. Dieser Ansatz wird dazu beitragen, die Beziehung der Partikeldispersion mit der turbulenten Flammenausbreitung zu verstehen und Versuche in einem größeren, ~1:5 skalierten Rohrreaktor mit 31 m Länge und 0.71 m Durchmesser vorzubereiten.

---

## Abstract

---

Explosions of coal dust in underground coalmines can be disastrous with multiple fatalities and massive property destruction. The explosion at the Upper Big Branch mine in West Virginia, USA, in 2010, caused 29 fatalities. This disaster has shown that coal dust explosions in underground coalmines can still occur if prevention measures are inadequate. Since the closure of the NIOSH Lake Lynn Laboratory, where the propagation of coal dust explosions was investigated, full-size physical test facilities for coal dust explosion prevention testing no longer exist in the United States. Full-scale testing is still possible in Poland (Barbara Experimental Mine), but this incurs high costs for traveling and conducting experiments. Scaled physical testing at  $1/5^{\text{th}}$  to  $1/50^{\text{th}}$  of full scale in combination with Computational Fluid Dynamics (CFD) numerical modeling helps scientists better understand the complexity of the multiphase chemical reactions, the thermodynamic mechanisms, and the turbulent fluid dynamics. Scaled testing with CFD creates realistic models to investigate the hazards and preventions of coal dust explosions in underground coalmines. The aim of this thesis is to investigate  $\sim 1/30^{\text{th}}$  scaled methane and coal dust explosions for the validation of CFD models. The tests were conducted in a 63 mm-diameter x 1.5 m, horizontal cylindrical steel reactor. The volume of the reactor used was 4.8 L. A series of tests were performed with different coal dust concentrations deposited on a metal plate inside the reactor. Sensors measured the flame speed and pressure at various points along the reactor. Initial results showed that the heat produced by the flame was too small to evolve the volatile matter of the coal dust particles. The coal dust absorbs the heat and decelerates the flame because the coal dust particles were exposed to the flame for too short a time. Tests using pre-dispersed coal dust were carried out under the hypothesis that the presence of a combustible dust cloud will increase the flame velocity in a methane-air mixture. The dust was injected into the reactor just before the methane-air mixture was ignited.

The second objective of this thesis was to design and build a reactor with a longer reaction zone for the coal dust particles. The second reactor is 1.5 m long with sidewalls of Plexiglass. This allows for visual examination of coal dust particle entrainment and interaction with the methane flame. Further research will be conducted with this reactor to understand the dynamics of the dust movement and the combustion of the coal particles. This approach will help us understand the coupling of particle dispersion with turbulent flame propagation and to determine design parameters for a larger, ~1:5 scale reactor that is 31 m long and 0.71 m in diameter.

---

## Table of content

---

Ehrenwörtliche Erklärung .....	II
Danksagung / Acknowledgements .....	III
Zusammenfassung .....	IV
Abstract .....	VI
Table of content.....	VIII
1 Introduction .....	1
2 Background .....	3
2.1 Mine disasters due to coal dust explosions .....	3
2.2 Coal dust explosion hazards .....	6
2.3 Coal dust explosibility .....	8
2.4 Main parameters of coal dust explosibility .....	11
2.4.1 Volatile matter of coal dust .....	11
2.4.2 The fineness of coal dust .....	12
2.4.3 Incombustible solid matter .....	13
2.4.4 Coal dust explosive limits .....	13
2.4.5 Free Water .....	14
2.4.6 Ignition Energy .....	14
2.5 Prevention of coal dust explosions .....	15
2.5.1 Prevention or Limitation of coal dust formation .....	16
2.5.2 Prevention of the dispersibility of the coal dust to form a cloud .....	17
2.5.3 Prevention of ignition of the coal dust .....	17
2.5.4 Prevention of the propagation of explosions .....	17
2.5.5 Passive and active barriers .....	18
2.6 Rock dusting method in the United States .....	20
2.7 The hygroscopic salt method practiced in European coal mines .....	22
2.8 Issues of dry and wet rock dust deployment .....	24
2.9 Coal dust testing in experimental reactors .....	24
2.9.1 Large-scale explosion test facility in China .....	27
2.9.2 Large-scale explosion test facility in Australia .....	28
2.9.3 Large-scale explosion test facility in South Africa .....	29
2.9.4 Laboratory-scale and large-scale explosion test facility in the U.S. ....	30
3 Experimental setup and investigation of coal dust explosion propagation	31

3.1	Experimental setup of combustion reactor .....	31
3.1.1	Steel reactor design .....	33
3.1.2	Sensor Technology .....	34
3.1.3	Coal dust specifications.....	36
3.1.4	Ignition system .....	37
3.2	Conduction of the coal dust explosion tests in the steel reactor.....	39
3.2.1	Results for methane-air explosions .....	40
3.2.2	Results of the obstructed reactor with the metal plate.....	42
3.2.3	Impact of the deposited rock dust.....	43
3.2.4	Impact of the deposited coal dust.....	44
3.2.5	Effect of deposited coal dust with different concentrations.....	47
3.2.6	Impact of the dispersed coal dust.....	49
3.2.7	Effect of pre-dispersed dust .....	54
4	Experimental reactor with rectangular cross-section.....	56
5	Conclusions and recommendations for future work .....	58
6	References.....	60
7	List of figures.....	65
8	List of tables .....	68
9	List of abbreviation .....	69
	Appendices.....	I

---

# 1 Introduction

---

In underground coal mines, coal dust and methane are produced from the mining processes of coal seams. Coal dust particles deposit on the entries, including the roof, rib, and floor areas, and can cause an explosion if they are entrained and ignited. In underground coal mines, fine coal particles that are produced from cutting processes can induce an explosion when entrained and ignited, for example, initiated from a methane explosion (Man et al. 2010). Several disasters of mine fires like the explosion at the Upper Big Branch which caused 29 fatalities in 2010 and the Jim Walter No. 5 mine which killed 13 miners caused a high number of fatalities in underground coal mines in the United States which illustrates that coal dust explosions can occur if measurements for prevention are inadequate. The current preventions are reflected by the regulation 30 CFR §75.403, where a minimum of 80 % incombustible content is required to prevent a coal dust explosion, which has to be continuously spread throughout the mine drifts. Whereas, Europe, South Africa, and Australia deploy active and passive barriers in underground coal mines to prevent coal dust explosions from propagating through the mine. Due to the different room-and-pillar layout of the mines and different sized and number of entries, the barrier system cannot be implemented in U.S. mines. Since NIOSH closed the Lake Lynn Laboratory for full-scale physical testing, there is no longer a facility available for suitable coal dust explosion tests in the U.S. However, scaled laboratory and field tests in combination with numerical models can reliably reproduce results of full-scale mine tests to investigate the behavior of coal dust in relation to methane gas explosions. Coal dust explosions can be controlled by adding rock dust in the intake and return air courses through passive and active explosion barriers and by coating the mine walls with hygroscopic salt solutions that bind the coal dust (Man et al. 2010).

Full-scale coal dust explosion testing is cost and time-intensive, noisy and produces a lot of smoke and dust. In order to mitigate these safety and health hazards, researchers believe that scaled laboratory tests of methane and coal dust explosions combined with Computational Fluid Dynamics (CFD) numerical modeling can replace full-scale testing. Advanced CFD modeling linked to scaled physical modeling is a proven approach to study the combustion and explosion

processes in power plants and internal combustion engines. Such testing, when applied to mine construction, can result in a full understanding of the complex reaction mechanisms and causes of methane and coal dust explosions in underground coal mines. Such an understanding could lead to the development of new methods of modifying and adapting existing barrier technology to the specific dimensions and layouts of U.S. underground coal mines. Rock dust and other extinguishing substances could be used in the prevention, mitigation, and suppression of coal dust explosions and to minimize the propagation of such explosions through underground coal mines. Researchers at Colorado School of Mines (CSM) have extensive experience in designing and simulating methane/ air explosion CFD models of longwall coal mines. The expertise is necessary to fully understand the chemical reaction between the homogeneous phase of methane-air with the volatile matter content of the coal dust particles.

The research in this thesis specifically aims to develop various experiments that simulate methane/ air/ coal dust deflagration under different mine conditions. Additional coal dust as a second reactive substance requires significant development of further CFD models. Therefore, this research will provide a beneficial approach and data to help researchers at CSM with further large-scale explosion tests, improving the chemical and physical understanding of the reactions that occur when methane and coal dust combust and the dynamic behavior of the dispersed coal dust particles.

The advanced shockwave of such an explosion whirls up more coal dust, which, in turn, settles on the surface, thus further feeding the flame. The presence of methane in the air reduces the lower explosive limit of the coal dust. For the purpose of studying the behavior of the methane and coal dust interaction, the laboratory-scaled steel reactor (153 cm length and 6.3 cm diameter), which was used for former methane/air explosion tests, will be modified to investigate the deflagration of different concentrations of coal dust. The behavior of the explosion will be measured with two different measurements. Ion sensors are going to be used to calculate the velocity of the flame, and pressure transducers record the pressure wave. To demonstrate the impact of various coal dust concentrations on the flame velocity and pressure wave, each parameter (methane mixture, the volume of the

methane mixture, ignition energy, air humidity, coal dust type, and size distribution), which influences the reaction must be considered.

Another goal presented in this thesis is the planning and construction of a laboratory-scaled reactor with a rectangular cross-section. The sidewalls of the reactor are made of plexiglass to provide images of the entrained coal dust particles dispersed from the blast wave as well as the burning of the particles as the methane flame passes the coal dust zone. Based on the images, it can be determined at which velocity and temperature the coal dust will be capable of propagating. This gives an insight into the impact of the run-up length up to a fully developed dust explosion. Data on pressure, temperature, gas and particle velocities, gas compositions, and flame propagation velocities will be recorded and analyzed.

---

## **2 Background**

---

### **2.1 Mine disasters due to coal dust explosions**

---

An explosion of coal dust in an underground coal mine has the potential to propagate through the mine, resulting in multiple fatal injuries and massive damage to the mine and the equipment.

There have been several explosion incidents in the United States and internationally over the past 40 years, which have contributed to the deaths of coal miners. Since the 1970s, U.S. Mine Safety and Health Administration (MSHA) statistics show 16 mine explosions in U.S. coal mines that have caused a total of 206 deaths, and since 2001, 59 deaths have been caused by coal dust explosions in U.S. underground coal mines. These numbers include the catastrophic explosion at the West Virginia Upper Big Branch (UBB) Mine with a loss of 29 miners and two seriously injured miners (Brune & Goertz, 2013; Schafner, 2018).

The 2010 UBB Mine disaster confronted America with the death of 29 miners and two seriously injured miners as a result of the devastating and violent nature of a coal dust explosion. The catastrophe was declared the worst mining accident in the last four decades that the U.S. had seen. Initially, the UBB explosion started as a small explosion of methane-air in the tailgate region of the longwall face, as described in the investigation report by MSHA. (Page et al., 2011). MSHA

investigators determined that the explosion occurred as a result of violations of fundamental safety standards, including inadequate face ventilation and inadequate amounts of rock dust applied throughout the mine.

The MSHA examination concluded that the volume of methane involved in the initial methane-air explosion may have been about 85 m<sup>3</sup>. The methane sensors at the tailgate and on the shearer body did not detect the presence of methane and, as a result, power to the shearer was not switched off automatically; something which should have happened at or above a methane concentration of 2.0 %.

Due to its estimated initial size, the methane explosion itself would have been located in, and its impact limited to, the immediate longwall and tailgate area where only a small number of miners worked. The methane-air mixture was most likely ignited by a frictional smear of hot metal from a dull cutter bit and malfunctioning dust sprays on the tailgate cutter drum of the shearer. The pressure wave of the local explosion dispersed loose, fine coal dust, which was in turn ignited by the initial methane explosion. This major coal dust explosion then propagated throughout the northern area of the mine. Based on the MSHA investigation, this fortify coal dust explosion travelled through about 67 km of mine workings. Along with a longwall and two continuous mining sections, this explosion destroyed the entire northwest production area of the mine (MSHA, 2012).

The explosion occurred as a result of the failing of or inadequate preventions, which were inappropriately implemented (MSHA, 2012):

- Several cutting bits were worn off at the shearer's cutting drum, and the operator had taken off several water sprays. The lack of water on the cutting surface led to the heating up of the cutting bits and hot smears. These are believed to have been the source of ignition for the methane-air explosive mixture.
- The ventilation system at the longwall was not sufficient enough to dilute and reduce the concentration of the methane, which accumulated next to the shearer. The roof support at the tailgate may have limited the amount of air along the face of the longwall.
- It was well-known that the explosion areas, in particular, the belt entries, were not sufficiently covered with rock dust to stop the propagation of the explosion. MSHA inspectors and UBB's own mine examiners had

recorded insufficient amounts of rock dust for several days prior to the explosion. The UBB mine examiners had found multiple belts that did not comply with the requirements for rock dust regulation. After the accident, MSHA investigators found that 90.5 % of the mine dust samples analyzed did not comply with the minimum of 80% inert by weight (MSHA, 2012).

Another fatal coal dust explosion in an underground coal mine happened in the Jim Walter No. 5 Mine, which is located in Alabama. In 2001, two separate explosions occurred and resulted in the death of 13 miners and three miners being seriously injured.

The first explosion was caused by a roof fall at the intersection of entry No. 2 in Section No. 4. The roof fall released methane into the mine atmosphere and damaged a battery charger at the intersection. The first explosion fatally injured one miner and destroyed several critical ventilation controls in Section 4, compromising the ventilation system and causing methane to build up. The second explosion was caused by an energized block light system in the track entry No. 2, which ignited the accumulated methane and resulted in a coal dust explosion. 12 miners lost their lives at this second explosion.

The incident was due to a failure to correctly assess the severity of the worsening roof conditions. The failure to maintain the incombustible content of rock-polluted surfaces in accordance with regulations contributed to the severity of the accident and the failure to identify these conditions during pre- and on-shift tests. The inability of mine management to undertake an entire mine-wide evacuation and the failure to de-energize all electrical circuits entering section No. 4 after the first explosion contributed to the severity of the accident (MSHA, 2003).

Every year many methane ignitions occur in U.S. coal mines. MSHA reported 34 “Gas and Dust Ignition or Explosion” events in 2011. Each of these ignition actions has the potential to trigger the propagation of a coal dust explosion similar to what happened in UBB (Brune & Goertz, 2013; Goertz et al., 2013).

---

## 2.2 Coal dust explosion hazards

---

Gas and coal dust explosions are basic hazards in coal mines. Such explosions have resulted in numerous deaths and injuries to miners as well as damage to and destruction of mining infrastructure and equipment. If the explosion of methane disperses and ignites the coal dust that has deposited in the mine, the explosion becomes immeasurably strong (Cashdollar et. al., 2006; Cybulski, 1975). Such a coal dust explosion can occur when a combination of several factors are present, which are (Amyotte et. al., 1993; Cybulski, 1975; Michelis, 1998):

- The concentration of methane in the mine atmosphere
- Presence of an ignition source
- Development of a localized methane-air explosion
- Formation of a coal dust cloud generated by the shock wave of the methane explosion
- Ignition of the suspended coal dust-air mixture
- Additional turbulent acceleration which raises more coal dust
- Propagation of a dust explosion throughout the mine

However, the presence of these condition does not necessarily lead to an explosion. Only when the respective limits are met, an occurrence of an explosion is possible (Michelis, 1998).

Requirements for coal dust to participate in an explosion include volatile matter, coal dust particle size, and the amount of coal dust available (Stephan, 1998). Due to the mechanization of mining processes, such as winning and transportation, the amount of coal produced has increased, leading to an increase of coal dust in the working area and along belt conveyors and transfer points. Also, mechanization resulted in a decrease in the coal particle size (Cybulski, 1975; Lacey, 1921; Sapko et al., 2006). On average, the mining coal liberates an average of 40 grams of coal dust per metric ton of coal mined (Luo et al., 2017). Finer coal dust particles remain in the air longer than the coarser particles and are, therefore, transported into the return airways before they settle (Sapko et al., 2006). The size of the fine coal dust particles that participate in an explosion is typically  $< 74 \mu\text{m}$  (Barone et al., 2017). Particle size surveys conducted in 61 mines showed that the amount of fine ( $< 74 \mu\text{m}$ ) coal dust from 20 % in the 1920s to 38 % in 2007 (Goertz et al., 2013; Sapko

et al., 2007). This increase is likely caused by a higher degree in equipment mechanization.

A methane explosion is, in most cases, the initiator of a coal dust explosion. In order for a methane explosion to occur, several conditions must occur. These include the minimal volume and the concentration limits of methane. The condition for the minimum volume of methane to initiate a coal dust explosion was determined at the Bruceston Experimental Mine (BEM) in 1930. Further investigations were done in the Lake Lynn Experimental Mine (LLEM) of the NIOSH Pittsburgh Research laboratory. The minimum amount of methane to disperse and ignite pure coal dust is  $0.4 \text{ m}^3$ , which is the result of the BEM and  $1.0 \text{ m}^3$  of the LLEM. The difference in the volume is due to the varying cross-section of the two mines (Cashdollar & Sapko, 2006).

Coal dust explosions are typically triggered by a primary methane explosion. For methane, the explosive limits are approximately 5 % for the lower explosive limit (LEL) and approximately 16 % for the upper explosive limit (UEL) (Cashdollar et al., 1996). The LEL of the methane changes in the presence of coal dust (Cybulski, 1975; Sapko et al., 2006). Figure 1 represents the limits of the flammability of a methane and coal dust mixture.

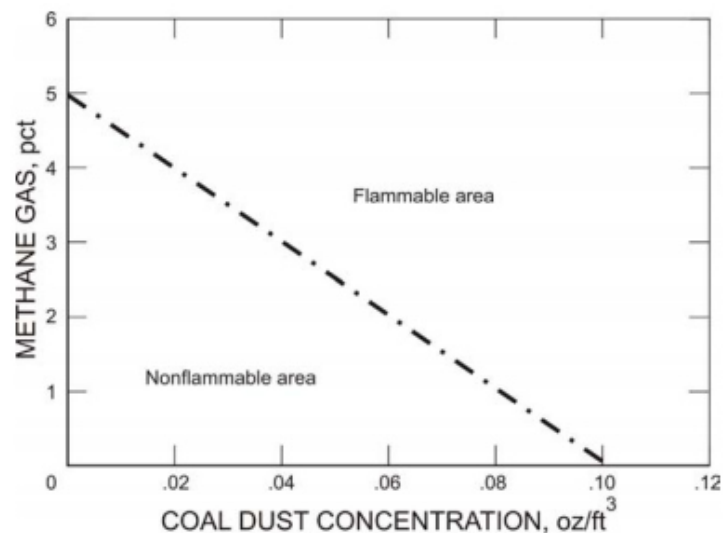


**Figure 1: Flammable limits of a methane-air-coal mixture (Cashdollar & Sapko, 2006)**

The flammable area for this mixture is above the dashed line, and the non-flammable area is below the line. The diagram shows that the LEL of methane

is 5 % without coal dust and decreases linear with of coal dust present (Cashdollar & Sapko, 2006).

In coal mines there is a variety of different ignition sources that can cause a methane explosion. The gas can be ignited by rock-on-rock or steel-on-rock frictional sparks, electrical sparks and arc flashes, open flames from burning coal, smoking or flame cutting and welding, and flames from explosives (Stephan, 1998). These are the most common sources of methane ignitions, but there are also some less common sources: hot equipment exhaust manifolds, sparking from certain metal alloys, or adiabatic compression (Kissel, 2006).

In many coal mines, the probability of the right combination of conditions for the ignition and the propagation of an explosion is relatively low. Once, a coal dust cloud is ignited, and heat is produced more quickly than can be dissipated to the environment, the contiguous coal particles will ignite, and the flame expands throughout the dispersed dust. This chain reaction leads to a rapid increase in pressure and temperature which, in effect, results in shock waves traveling throughout the openings of the mine. The coal dust present on the floor and the ribs will be elevated and scattered through the air rush and turbulences will be generated by the explosion, thereby allowing expansion of the explosion (Cybulski, 1975).

---

## **2.3 Coal dust explosibility**

---

Investigations concerning the explosibility of coal dust determine its capability of propagating explosions. Coal dust in mines is dangerous only if it is capable of propagating explosions. The theory of coal dust explosions can be divided into three parts relating to the following problems:

- The ignition of coal dust
- The propagation of a coal dust explosion
- The formation and development of coal dust explosions in mine workings

An explosion may propagate because dust particles, yielding tar and gaseous substances, radiate very strongly during ignition and may cause the propagation of the coal dust explosion, which means the volatile material content of the dust evolves (Cybulski, 1975). Strong initiators can also directly cause very fine coal dust particles to ignite (NIOSH, 2011; Cybulski, 1975). The ignition happens because of the rapid movement of radiating dust particles which are dispersed in the

atmosphere (Cao et al., 2014). The dispersed particles act as an ignition source and propagate the reaction in the dust and air (Ajrash et al., 2017).

The chemical and physical processes are more complex in coal dust explosions than in the case of pure methane explosions (Cybulski, 1975; Lacey, 1921; Si et al., 2012). In addition to a solid phase, the dispersed coal dust contains a gaseous phase. To create conditions under which an explosion can occur, coal dust needs to be dispersed in air, which requires a certain amount of energy. Turbulence of coal dust explosions controls the dispersion of coal dust and the propagation of explosions. To distribute a sufficient amount of dust, a certain flame velocity must exist. Below the concentration limit, an explosion cannot develop because the flame velocity and turbulent energy is insufficient to sustain the explosion (Cybulski, 1975; Mishra & Azam, 2018).

Flame speed is a critical parameter for the coal dust explosions. Coal dust explosions may occur by deflagration or detonation. The flame energy of the initial methane explosion depends on the percentage of CH<sub>4</sub> content in the atmosphere (Ajrash et al., 2017a). The flame velocity of a methane explosion depends on some basic parameters (Cybulski, 1975; Kundu et al., 2016):

- Composition of the explosive mixture and concentration of the methane
- Conditions of the expansion of the combustion products of CH<sub>4</sub>
- Characteristics of the initiation
- The condition of working and cross-sections
- The accumulation quantity of the explosive methane mixture

Under these parameters, the flame velocity of an explosive methane mixture fluctuates between several and 800 m/s of approximately stoichiometric composition (Cybulski, 1975). Experiments in a detonation tube at the Lake Lynn Laboratory resulted in an average flame velocity in the range of 750 m/s to 900 m/s, the lower and upper flammable limit of methane (Zipf et al., 2013). The turbulent movement in methane explosions is significant. Due to turbulence, the velocity results in a marked increase as it consumes a higher volume of methane. For example, the resulting velocity and violence of the explosion are much higher when the same explosive methane mixture under the same conditions is ignited by shot firing rather than by an electrical spark (Cybulski, 1975; Zipf et al., 2013).

The coal dust concentration in the atmosphere normally varies in the working cross-section. Even in laboratory conditions, a consistent concentration of coal dust is difficult to maintain. Under certain mining conditions, a cloud of coal dust is a dynamic and heterogeneous system and is typically in a state of chaotic movement. Generally speaking, the spread of the explosion is suspected to occur as a result of the explosion wave that produces sufficient dust cloud concentration in a cross-section of the mine (Cybulski, 1975).

Cybulski (1975) stated that the characteristics of the explosibility of coal dust in a closed system are described as the maximum pressure, along with the maximum and average increase of the pressure rate formed during the self-sustained combustion of the clouds. The degree of the explosibility also depends on the following variables (Cybulski, 1975; Roychowdhury, 1960):

- Composition of the dust, which includes volatile matter, moisture and ash content
- The particle size and size distribution of the coal dust
- Shape and surface characteristics of the dust
- Presence of inflammable dust in the atmosphere
- The concentration of dust raised to form the cloud
- Distribution of the dust in the various parts of the mine
- Nature and strength of the source of ignition
- The oxygen content of the dispersion medium and the nature of the remaining constituents
- The uniformity of dispersion of dust in the cloud
- The fraction of the potential heat of the dust which is liberated during an explosion and the temperature and pressure of the dust cloud before ignition
- Surrounding conditions which affect the rate at which energy is taken from the ignited dust, either by direct absorption of heat or by the release of pressure
- The age of the dust, as it dries out while exposed to air.

The criteria for the lower limits of the explosibility in which self-propagating combustion still occurs are the minimum concentration of coal dust, the minimum ignition energy, and the lowest limit of the oxygen concentration (Cashdollar, 1996).

---

## 2.4 Main parameters of coal dust explosibility

---

According to Cybulski (1975), the main parameters which play an important role in the explosibility of coal dust are the volatile matter, the fineness of the coal dust, the content of incombustible solid matter, the amount of coal dust, the content of free water which acts as an incombustible matter and the effect of the time of deposition of coal dust.

---

### 2.4.1 Volatile matter of coal dust

---

The evolution of the volatile matter is a result of the thermal decomposition of the coal without air exposure. While the air has access to dust particles in the event of a coal dust blast, the evolution of the explosive substance creates pyrolysis during which the chemical and physical coal composition is subject to a transformation. The liquid and gaseous solutions are formed during pyrolysis, and coke persists (Merrick, 1983).

The difference in weight of coal before and after being heated to about 1120 K (850 °C) under defined conditions indicates the volatile matter material. The volatile matter is the result of chemical reactions, namely the thermic decomposition of coal and many other reactions between products without the access of air. Liquid and gaseous substances evolve throughout the pyrolysis (Cybulski, 1975). The volatile matter is usually calculated by comparison to the dry ash-free coal substance (Parr, 1911). This magnitude is a distinctive and significant parameter of coal in the question of the explosibility of coal dust (Cashdollar, 1996; Cybulski, 1975; Lacey, 1921; Roychowdhury, 1960; Stephan, 1998).

The evolution of volatile matter of coal dust is of paramount importance under the impact of high flame temperatures. When a thermal source of sufficiently high temperature occurs in a cloud of coal dust, it first induces the evolution of volatile matter from coal dust (Merrick, 1983). The evolution also depends on the degree of fineness and the particle size of the coal dust. The volatile matter of particle with a specific surface of 1000 g/m<sup>2</sup> is burned after 1.4 ms, while the same process takes 7.6 ms for a particle with a specific surface of 510 g/m<sup>2</sup> (Cybulski, 1975).

The volatile ratio was defined by the former US Bureau of Mines to determine the explosiveness of coal. Laboratory analysis measures the reactive content and fixed

carbon concentrations of the coal as well as moisture and ash. The volatile ratio is calculated as the volatile matter divided by the amount of fixed carbon and volatile matter. Coal dust with a volatile ratio above 0.12 has been found to pose a risk of dust explosion. This category includes all bituminous coals except anthracite. Anthracite coals, by definition, have a volatile ratio of 0.12 or less and are not a risk for explosions. It is important to note that fire can occur with either bituminous or anthracite coals, but only bituminous can be associated with explosions (Nagy, 1981; Stephan, 1998).

---

#### **2.4.2 The fineness of coal dust**

---

As stated above, another important requirement is the fineness of the coal dust. The influence of the grain size on the course of the explosion can be generally stated in the following way: the finer the coal dust, the more violent the reaction process, whereas the coarser the coal dust, the slower the reaction process (Cashdollar, 1996; Man et al., 2010).

Hence, the degree of fine dust in mining operations must be well known, due to the importance of the fineness of carbon dust in terms of the explosibility of coal dust. In addition, the dispersibility of the coal dust increases significantly with the rise in the degree of fineness of coal dust (Cybulski, 1975).

Experiments showed that dust particles moving through a standard 20-mesh U.S. regular sieve (850  $\mu\text{m}$ ) would take part in an explosion of coal dust. U.S. Bureau of Mines research determined that coal dust with a particle size greater than 850  $\mu\text{m}$  do not contribute to a coal dust explosion. The finer the particle size, the more violent the explosion. For pulverized fuel systems and fluidized bed reactors in thermal power plants, the feed coal is typically reduced to a particle size >85 percent passing a 200-mesh U.S. standard sieve with 74  $\mu\text{m}$  openings. Smaller coal dust particles require less energy to ignite. Thus, heat transfer rate between finer particles is faster than between coarse particles, resulting in higher pressures and more rapid pressure increases during an explosion (Harris et al., 2015; Stephan, 1998).

---

### **2.4.3 Incombustible solid matter**

---

The incombustible solid matter can be derived in four different origins: the ash content consisting in the coal; the hygroscopic water; the crushed rock from the roof, and the floor; the rock dust (usually limestone) added to the coal dust under regulation requirements (Cybulski, 1975). The role of an incombustible solid matter is to prevent the propagation of coal dust explosions. The higher the content of incombustible solid matter, the lower the explosibility (Azam et al., 2019; Harris et al., 2009).

An increase in the amount of stone dust contained in coal dust makes the burning of it more intricate as the heat from the combustion is largely used for heating the stone particles. In the case of a cloud of coal dust containing stone dust, a portion of the heat produced by the combustion of coal dust is also transferred to solid incombustible matter, making it more difficult, naturally, to develop the flame in the coal dust cloud (Cybulski, 1975).

However, the most crucial role of incombustible solid material in a coal cloud is to shield the particles of coal dust from the radiative heat emitted by the combustion reaction of volatile matter and coke. The heat energy is transmitted by radiation most easily and quickly. It is precisely this process of the transfer of heat energy that dominates the explosion of coal dust. In a mixture of coal and stone dust, the particles of incombustible solid matter protect the particles of coal dust from the radiated heat. The importance of the role of radiation in the process of a coal dust explosion is demonstrated by the fact that, to prevent coal dust explosions from propagating, very high levels of over 80 % of incombustible solid matter are necessary (Luo et al., 2017).

---

### **2.4.4 Coal dust explosive limits**

---

Another essential criterion for the explosibility of coal dust refers to the available concentration, defined as the lower explosive limit (LEL). It is the minimum amount of coal dust in suspension that is capable of propagating and which can create enough energy to cause damage (Cashdollar, 1996). The LEL is about 100 g/m<sup>3</sup> for deposited bituminous coal. When the coal dust is already dispersed, the lower limit of the explosive concentration is about 60 g/m<sup>3</sup> (Michelis, 1998; Stephan, 1998).

The minimum thickness of an explosive layer of coal dust at deposited on the mine floor is about 0.13 mm or about the thickness of a sheet of paper (Nagy, 1981).

The upper explosive limit is not well-defined. Researchers found that the flame front velocity is low when a coal dust concentration of 3800 g/m<sup>3</sup> is used and that an explosion with concentrations above 5000 g/m<sup>3</sup> would quench within 3 m. of the ignition source. The involvement of ash, rock dust, or inert gases can reduce the hazard of the LEL of the coal dust (Stephan, 1998).

---

#### **2.4.5 Free Water**

Moisture or free water is usually present in underground coal mine dust. The humidity has to be often considered due to its specific influence on the explosibility of coal dust. It be noted that hygroscopic water is treated as an incombustible solid matter and should be discerned from free water. Hygroscopic water is important to prevent the entrainment of coal dust explosions but is only effective if the content is very high. Other than that, the content of free water doubles the effect of decreasing the explosibility of coal dust. Water in sufficient quantities decreases mine dust dispersibility. It impedes the dust from lifting to the surface and dispersing to a cloud that is capable of propagating an explosion (Cybulski, 1975).

---

#### **2.4.6 Ignition Energy**

Another important consideration is the energy of the initiator of the explosion. With the rise in energy generated by the initiating explosion, the capacity to disperse coal dust also increases. The amount of heat produced by the initiator and the degree of its impact on dust plays an important role. It is challenging to ignite coal dust using a relatively weak initiator, while the same coal dust will cause a very violent explosion if a potent initiator is used (Cybulski, 1975). Experiments have shown that, in the absence of methane, frictional sparks can directly ignite a coal dust cloud. The minimum ignition energy (MIE) of coal dust clouds is 30 mJ to 60 mJ (Michelis, 1998) and depends on oxygen content, volatile matter, the fineness of the coal dust, the coal dust concentration and the moisture content (Stephan, 1998). For comparison, the minimum ignition energy of methane at standard conditions is 0.28 mJ at a near-stoichiometric concentration of 8.5 % (Michelis, 1998).

---

## 2.5 Prevention of coal dust explosions

---

The focus of this chapter is to describe the general application of preventative measures against coal dust explosions, the rock dusting methods and regulations in the United States as well as the hygroscopic salt method which is practiced in German coal mines, the contrast between these prevention methods and the issues of the deployment of rock dust as a slurry or foam.

Measures to prevent explosions underground can only be as effective as their application allows. Each measure in itself is only one component of the overall protection system. It is not feasible to design and operate this system in such a way that an explosion accident can be entirely ruled out. There is always a residual risk. However, even in situations in which an explosion event occurs, the effects should be reduced to a minimum, which is the task of the explosion protection.

Figure 2 shows a schematic overview of explosion prevention and the different application and methods used to prevent a coal dust explosion. In the first place, the measures are focused on preventing the formation of coal dust and methane. On the other side of the diagram there are constructive measures. These are some protection zones against further propagation of a coal dust explosion. They include explosion barriers, which will be discussed later, explosion stoppings and special structures. Only the deployment of both preventive and constructive protective measures makes it possible to maintain a safe mining operation (Du Plessis & Saleh, 2017).

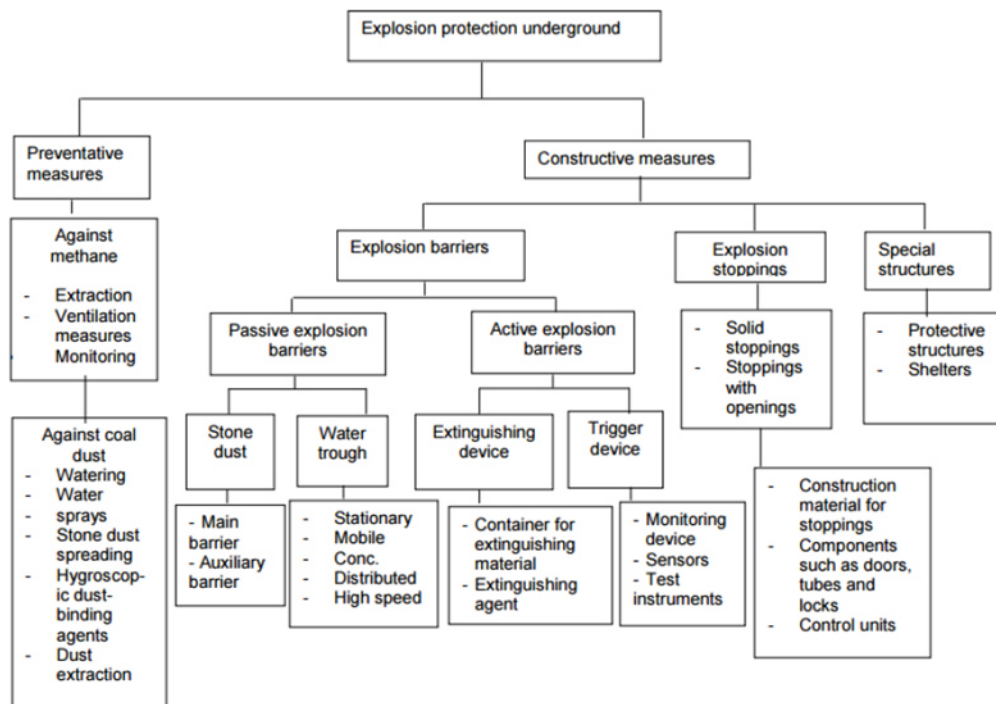


**Figure 2: Schematic of different explosion preventions and the methods and applications behind it**

The preventative measures against coal dust explosion include (Cybulski, 1975; Lacey, 1921):

- Prevention/ limitation of coal dust formation
- Prevention of the dispersibility of the coal dust to form a cloud
- Prevention of ignition of the dust
- Prevention of the explosion to propagate.

### 2.5.1 Prevention or Limitation of coal dust formation

The formation of coal dust in mines cannot be avoided, but there are some technologies to reduce the formation of coal dust.

In mechanical coal production, when machines with cutting elements are used (e.g. continuous miner, longwall and crushers), the formation of coal dust is relatively high. One method to limit coal dust is to decrease the movement of the cutting elements (Cybulski, 1975). Another and more common method is the use of water sprayers placed on the equipment to reduce the airborne coal dust (Goertz, 2017). Experiments have shown that foam suppression techniques suppress dust concentration 30 % more efficiently compared to water-spraying methods at conveyor belts (Liao et al., 2018).

---

### **2.5.2 Prevention of the dispersibility of the coal dust to form a cloud**

---

When the coal dust is dispersed in air with sufficient concentration, it becomes an existing hazard, which can lead to a coal dust explosion (Cybulski, 1975). As mentioned in section 2.4.5, a method of effectively preventing the dispersion of coal dust is the use of wetting and binding agents. If the amount of water is high enough, the likelihood of an explosion decreases.

---

### **2.5.3 Prevention of ignition of the coal dust**

---

In the United States, electric equipment used underground must be certified by MSHA as “permissible” for use in mines (Brune et al., 2007). This preventive measure comes into play in the event of blasting. Before shooting, spraying the faces with water or stone dust only serves as a practical purpose. The coal dust should be flushed down to the ground by water primarily from the upper parts of the drifts where the most harmful particles reside as it is more likely for these particles to be lifted by an explosion and form a dangerous coal dust cloud (Cybulski, 1975).

---

### **2.5.4 Prevention of the propagation of explosions**

---

One of the first practices in the mining industry to prevent coal dust from propagating is to bind coal dust with water. The system is successful only when coal dust, deposited during mine operations, is saturated by water in its entirety so that it cannot be raised into the air and dispersed even with the most powerful explosion likely to occur in the mine (Cybulski, 1975).

The application of rock dust as the incombustible matter has already been discussed in the previous chapter. Intensive research is being conducted on the application of rock dust. The principle of its application is straightforward. It consists of the admixture to coal dust of such a quantity of incombustible solid matter, which will make the dust incapable of propagating an explosion.

---

## 2.5.5 Passive and active barriers

---

Any of the preventions of coal dust explosions discussed above have a risk of failing. In the event of such failures, the coal dust explosions will propagate. Therefore, it is undoubtedly desirable to ensure that the course is as short as possible. Explosion barriers can suppress an explosion in the areas of active mining. In the circumstances, the possibility of both initiation and development of coal dust explosions must be taken seriously. Therefore, a certain measure must be used as the last line of defense of maximum dependability to control the range of an explosion. There are two different types of barriers: passive and active barriers.

### 2.5.5.1 Passive barriers

Passive barriers can either be stone dust or water barriers depending on the type of inert material used (Zou et. al., 2001).

The barrier absorbs the kinetic energy of the blast wave of the explosion. When the flame of the explosion arrives, the wave energy overthrows the barriers and disperses the inert material in the path of the fire. Water or stone dust should be dispersed entirely when the flame hits the barrier zone. If the shield is too far away or too close to the explosion source, the explosion might not get wholly extinguished. As a rule, the barriers should be mounted at least 60 meters from the face. On the other hand, they should be installed as close as possible to the source to prevent flames from spreading (Ng et al., 1987).

Several types of mines in South Africa, Europe, and Australia have been extensively studied and the use of passive barriers tested and successfully deployed. Two types were tested intensively by Polish and German institutions: Polish barrier (Figure 3) and the Dortmund barrier (Zou et. al., 2001).

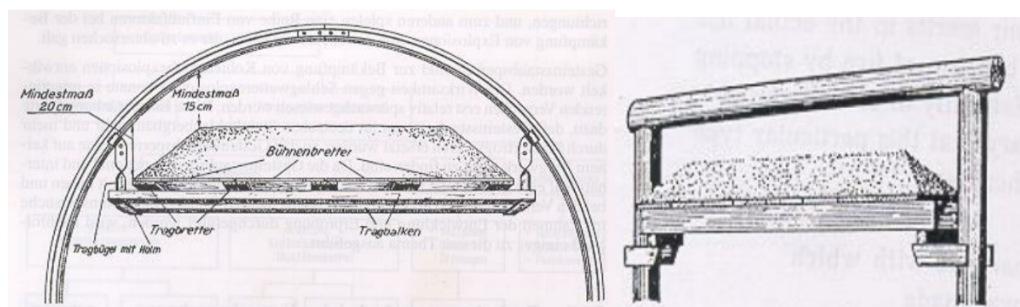


**Figure 3: Design of the polish stone dust barrier**

Passive water barriers work similarly to stone dust barriers. They are water-filled containers, such as troughs, tubs, and bags. The spilled water is dispersed through air turbulence and forms a barrier of water droplets through the fire path, which quenches the flame (Medic-Pejic et al., 2015).

Passive barriers face, in general, a few problems which can cause a failure if they are not frequently maintained. A disadvantage of passive barriers occurs when the explosion is too weak, or the barriers are too close to the explosion source. The kinetic energy of the blast wave is not strong enough to turn the shelves and disperse the inert material. In general, water barriers have some advantages over stone dust barriers. They are easier to maintain, easier to install, and cheaper compared to stone dust barriers. Also, high air velocity in the drifts, moisture, and time can cause issues for stone dust barriers. The dust can be blown off of the barrier from strong air currents. The stone dust tends to clump with time and in mines with a high moisture content, which makes the rock dust ineffective in case of explosion (Zou et. al., 2001).

#### **2.5.5.2 Active barriers**

It is challenging to ensure the correct time to trigger the passive barriers for the most effective suppression. Therefore, active barriers with trigger devices are built to meet the requirements. The objective is to predict the arrival of the flame front and to disperse inert materials at the correct time (Du Plessis et. al., 2017). The barriers triggered consist of three main components: the sensor, the dispenser, and the suppressant. The oncoming explosion is sensed by a sensor unit by increasing static pressure, temperature, or radiation, and the machine is used to trigger the dispenser. The distributor releases an inert material with compressed gas, a spring, or explosive material (Du Plessis, 2015).

Active barriers have significant advantages over passive barriers (Zou et. al., 2001):

- Suppressants are dispersed through an independent, self-contained source of energy.
- The function of an active barrier does not depend on the intensity or impact of an explosion.
- It is ideal for highways with a low height/width ratio where height is below 80 % of the width.
- It is appropriate for a rapidly advancing face.

- It offers an excellent safety standard because it responds to a full-scale explosion before the flame develops.
- The early stage of propagation can be detected.
- A small amount of carbon monoxide is produced.

However, active barriers also have a few disadvantages. In most coal mines, power in places where explosion protection is needed is difficult to supply. As a result, it may be difficult for some mines to implement it. However, battery-operated internal power supplies can overcome this problem. A further disadvantage of active barriers is that, once activated, the remaining coal dust is limited, and the initial inert zone is easily transversally affected by a secondary coal dust explosion (Zou et. al., 2001).

---

## **2.6 Rock dusting method in the United States**

---

The Code of Federal Regulations (CFR) 75.402 to 75.404 requires rock dusting in all underground bituminous coal mines in the United States. The percentage of rock dust should be no less than 80 % in the intake and return airways. The presence of CH<sub>4</sub> requires increasing the rock dust amount by 10 % in intake air courses and 4 % in return air courses if the ventilating air contains 1 % of CH<sub>4</sub>.

In addition, the potential hazard of a coal dust explosion can occur if the rock dust and the coal dust are not mixed well. The effectiveness of rock dust also depends on the fineness of the particle size. The Mine Safety and Health Administration (MSHA) requires a specific particle size distribution for rock dust. Defined by 20 CFR 75.2, 70 % of the particles have to pass a 200 mesh sieve (~ 74 µm). The rock dust regulation is also specified by 30 CFR 75.2, according to which the dust used must be 100 % less than 20 mesh (<850 µm) and 70 % lower than 200 mesh (<74 µm). It must contain no more than 5 % of combustible materials and less than 4 % free and mixed silica (SiO<sub>2</sub>). The dust layer should not compact to form a cake when wetted and dried out after (Perera et al., 2016).

The frequency and severity of coal mine explosions in the United States appear to be much lower after the U.S. implemented these safety measures in the 1920s and 1930s on the instruction of the U.S. Bureau of Mines. Figure 4 shows how the number of deaths decreased after rock dust regulations between the 1920s and 1930s were applied against coal mine explosions (National Academies of Sciences, Engineering, and Medicine 2018).

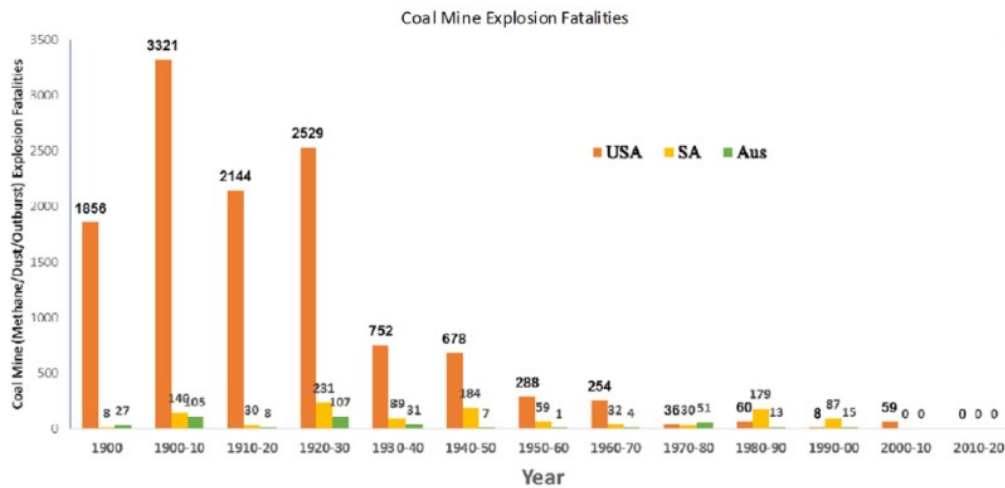


**Figure 4: Statistic of coal mine explosion fatalities from the 1900s (National Academies of Sciences, Engineering, and Medicine 2018)**

Previous research on a large scale and small-laboratory scale have shown that particle size is important for the performance of rock dust. The bigger the particle size of rock dust, the more rock dust is needed to inert the coal dust and prevent the explosion from spreading. Several small-chamber studies have shown that reducing the size of rock dust particles reduces the surface area of rock dust and facilitates greater absorption of radiant heat (Dastidar et al., 1997).

In the United States, two applications of rock dust in coal mines are permitted by regulation: application of dry and wet dust:

Dry rock dusting is performed pneumatically and performs better than wet dusting, especially in the case of an explosion in regard to lifting and dispersion of the dust due to the shockwave (National Academies of Sciences, Engineering, 2018) . Strict respirable dust laws can, however, conflict with the effectiveness of dry rock dusting. Dirt not adhering to the bare surfaces flows along the air path to the active area in which the mining workers work, while dry dusting takes place on the intake ventilation path. In 2014 a new dust regulation limited the volume of rock dust, which can be dispersed over a specific period. This rule tends to limit the production of the mine because miners are not to dust the newly exposed coal seam with rock dust on time, which also leads to an increase of coal dust that may become a hazard fuel in case of an explosion due to an improper volume of rock dust. Some mines have switched to wet dust in order to counteract respirable coal mine dust (RCMD) produced by dry dusting. Many activities have continued to comply with the dust law

of 2014 by not dusting when employees work at the face during production to reduce the exposure time for workers in the section where rock dusting takes place (National Academies of Sciences, Engineering, 2018).

Wet dusting means mixing dry dust with water and then spraying the mixture on surfaces of the mine. While this method initially mitigates the breathing dust problems of dry dusting, there is a new set of problems. Wet rock dust must dry up on surfaces before it can prevent the propagation of a coal dust explosion. Wet dusting typically often creates clumps of rock dust, which are called cakes. The clumped rock dust maintains some water, and, in case of an explosion, the dust will not disperse, to extinguish the flame front. Essentially, a whole new set of problems with wet dusting exists and may not prevent the propagation of coal dust explosions (Eades, 2016). Furthermore, several companies are developing technologies that include a mix of wet dust and additives, which allows the dried rock dust to become more friable and, therefore, dispersible. Companies are also working to prevent caking, thereby preserving particulate size distribution and dispersibility in different mine-atmospheric conditions in rock dust with chemicals including stearic acid, oleic acid, and sodium oleate (Huang et al., 2015).

---

## **2.7 The hygroscopic salt method practiced in European coal mines**

---

The European Union mainly uses hygroscopic salt solutions instead of rock dust in areas where coal dust can accumulate. The mining companies are expected to use hygroscopic dust binding agents in preventative explosion protection of underground hard coal mining. Hygroscopic dust binding agents for underground use must be approved. The approval is based on a test of the technological and safety properties performed by the fire and explosion protection specialist agency of the Tremonia experimental mine. Tests include durability, penetration, adhesion, ability to bind to dust, and velocity of dust (Michelis, 1996).

The hygroscopic salt can be used as powder, as a paste, as salt flakes or as a solution. Since coal dust is hydrophobic, the dust particles float on water and therefore remain airborne. In order to ensure that the coal dust sinks and are covered with the salt, a wetting agent is added to the salt to lower the surface tension (Goertz, 2017). The effectiveness of the dust binding agent depends on the coal

type, the grain size, the dust quantity, and the dust content. In addition to the deposited dust, the very fine coal dust suspended in the air is also bound. The efficacy and duration of the action of salts on airborne coal dust were examined in the 1960s. The aggressiveness of the salts is a disadvantage. Objects made of steel are susceptible to the highly corrosive nature of the salt, especially road lines and conveyor systems. The salts can also damage electrical equipment (Michelis, 1998). The most common applications at present are as a powder, paste, flakes, and solution. Pastes in their initial composition can bind dust for weeks until they are exhausted and have to be regenerated. Thus, pastes are as fluid as solutions. Recently, solutions have been increasingly used for reasons of practicality, which means shorter treatment intervals for the operation, as the ability to bind dust is now only guaranteed for days. The properties of solutions also apply to the use of powder (Michelis, 1996).

$\text{CaCl}_2$  and  $\text{MgCl}_2$  are the most commonly used salts. Each can be used in dry powder or prill form or as a solution of ~30 %. Surfactants can be applied to improve the hydrophobic coal dust adsorption and the time between spray treatment cycles (Goertz, 2017).

It must be remembered that the use of salts against rock dust has certain advantages (Goertz, 2017):

- Salts must be added every few days. They remain able to bind coal dust, and there are no problems with layering.
- Salts can be easily added to the ribs and roofs and structures such as wire mesh roof and cables.
- Salt may be used on-shift without affecting workers downwind.
- Salt is more efficient than rock dust as it requires smaller amounts.
- The salt application can be automated along belt conveyors and transfer zones by installing spray nozzles.

---

## **2.8 Issues of dry and wet rock dust deployment**

---

Since rock dust can disturb workers from dust applications, several companies offer wet and foam-based rock dust products. In September 2012, results of research were published by the National Institute for Occupational Safety and Health (NIOSH) which showed that hydrophobized limestone-based rock dust tended to cake when dried. In other words, the rock dust forms a hardened mass that cannot be dispersed by air and is, therefore, not effective in case of an explosion.

The particles of the water form a connection through cohesion and adhesion between the individual rock dust particles. These bridges allow the molecules to flow within the particles of rock dust. When particles of rock dust start drying, material suspended within the liquid bridge is recrystallized and creates a solid bridge between particles. When rock dust is exposed to a cycle of wetting and drying, solid bridges strengthen and decrease the space between the particles of rock dust, causing an agglomeration of particles (Christakis et al., 2006). This agglomeration is referred to as "caked" rock dust in the industry. The distinct clumps of rock dust can be recognized (Eades, 2016).

Similar problems occur with foam-based rock dust. The application of this type of rock dust has been explored for a long time. The dust of the foam rock has been deposited on the surface of the mine drifts. The foamed rock dust cannot be scoured off once the mixture is hardened. NIOSH has established that foam in the case of an explosion is not as effective as dry rock dust.

---

## **2.9 Coal dust testing in experimental reactors**

---

Insufficient methods to model structures of the coal dust cloud and flame propagation to predict the course and effect of coal dust explosions. To understand the characteristics of mining dust explosions and the complexity of it, these problems were studied at U.S. Bureau of Mines and the NIOSH's Lake Lynn Experimental Mine in the United States (Sapko et al., 1996), the experimental mine Tremonia in Germany (Michelis, 1998) and mine-scale coal dust tests in the Barbara experimental mine in Poland (Michelis, 1998) were performed to study the characteristics of mining dust explosions and other industries where dust explosions can occur.

Full-scale experiments are time-consuming and expensive (Fleming et. al., 1917). Experts have attempted to establish laboratory-scale tests, which can efficiently duplicate the outcomes of full-scale studies to save labor and capital (Liu et al., 2010).

Therefore, several laboratory experiments on explosions of coal dust and gas were conducted concerning the explosion of mining with a 1.2 L Hartman tank, a 20 L Siwek chamber (Cashdollar & Hertzberg, 1985), a 1.25 m<sup>3</sup> explosion chamber (Klemens et al., 2000), pipes in different sizes and vessel attached pipes (Ajrash et al., 2017; Liu et al., 2010). The characteristics of coal dust explosions in pipes vary from those in spherical vessels because of the different geometries and the L/D ratios (Liu et al., 2010).

USBM developed the first experimental system based on the Hartman Chamber with a volume of about 8 L. The Bureau originally constructed the tank for explosibility studies of homogenous gas mixtures (Eades et al., 2018). The nominal concentrations of these experiments were released where the coal dust mass was a fraction of the chamber volume (Hertzberg et al., 1979). Due to the minimal volume and the lack of dispersing the coal dust right before the ignition, a 20 L spherical chamber was designed by Siwek (Kalejaiye et al., 2010).

The USBM has used the 20 L capacity explosive chamber as the typical dust blast testing device ever since. A series of tests were performed by Cashdollar and Hertzberg using an explosive chamber (Cashdollar et. al., 1985). The coal dust was deposited on the bottom of the dust chamber in a tank. Pressurized air was dissipated from the nozzle into the chamber and dispersed the coal dust to achieve a comprehensive mixture of air-coal before the chamber was ignited (Kalejaiye et al., 2010).

Much laboratory data was obtained in the 20 L USBM vessel, which was widely used to analyze the explosiveness of coal and other carbonate dust (Cashdollar et. al., 1985). USBM researchers addressed different aspects of the explosibility of coal dust. These included the ignition energy requirement of specific measurements of flammability limits of dust and gas, a flame propagation model, volatility effects on coal and other carbon dust explosibility limits, the influence of particle size, comparisons of data from 20 L and 1 m<sup>3</sup> chambers, minimum concentration of

oxygen, requirements of rock dust to inert explosions of coal dust and laboratory-scaled and full-scaled data comparison (Eades et al., 2018).

Both Nagy (1983) and Bartknecht et al. (1981) reported that the LEL of a methane - coal dust mixture is lower than the LELs of methane or coal dust separately. Some researchers subsequently studied the risks and the flammability limits of mixed hybrid fuel using laboratory instruments. To prevent an explosion of coal dust, Nagy et. al. (1965) determined that at least 80 % of incombustible material is needed. The current regulation 30 CFR § 75.403 practically illustrates this. He also explains the fluid and static pressure produced during a coal mine explosion. Static pressure is formed by increasing products of combustion, it is equal in all directions, and is measured in closed volumes (Nagy, 1981).

Cashdollar published the explosive properties of coal dust and composite mixtures in several papers. The tests were performed in a 20 L vessel in which the ignitors were in the middle of the chamber. The risks of combustible dust and flammable gas mixes have been identified as being determined by the Over-Pressure Raise (OPR), deflagration index (Kst), flammability levels, minimum oxygen concentration and minimum ignition energy (MIE). Composition of coal dust and a methane concentration of only 2.5 % (below the flammable limit of methane) raised the explosion probability, which was shown by Cashdollar (Ajrash et al., 2016). Torrent observed in other experiments using the same instruments as Cashdollar and others that the overpressure rise of coal dust rose by 33 % when only a 3 % concentration of methane was applied. In laboratory and large explosion chambers, the effects of the initial ignition source on the explosion and fire property were studied (Torrent & Fuchs, 1989), and Cashdollar (1996) showed the influence of the ignition energy on explosion characteristics through the use of a 20 L vessel.

The literature review demonstrates that tests of methane and coal dust in large detonation tubes have not been observed quite so well. Liu et al., Arjash et al., and scientists of NIOSH and USBM are some of the few who researched methane and coal dust explosion properties in a large-scale detonation tubes. Furthermore, experiments by Bartknecht on coal dust and gas explosions were carried out in two laboratory tubes of separate diameters and lengths. Through the entire experimental tube, the dust cloud was created by injecting dust from a number of equally spaced external pressurized tanks. The coal dust air mixture was ignited by an explosive methane/air mixture bag.

### 2.9.1 Large-scale explosion test facility in China

Liu et. al. (2010) used a large horizontal tube reactor shown in Fig. 6. The tube has an internal diameter of 200 mm and a length of 30 m. Various tests performed in this tube analyzed pressure and velocity wave of the coal-dust explosion, effect of dust particle sizes, impact of the dust concentration, and influence of the volatile matter.

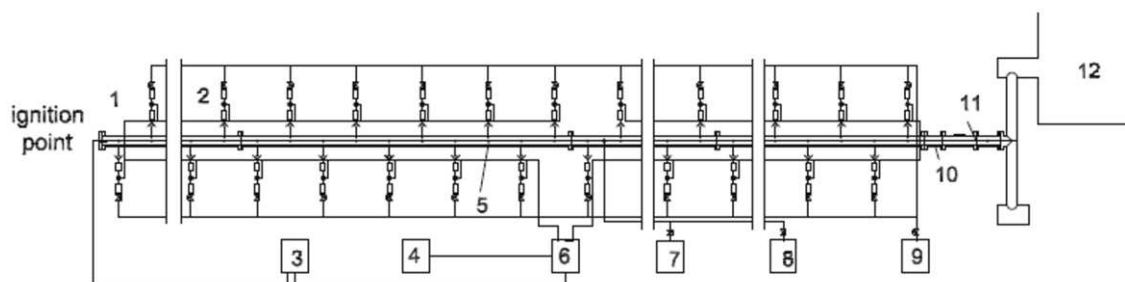


**Figure 5: Schematic drawing of the experimental set-up of Chinese reactor: 1) experimental tube, 2) dispersion system, 3) ignition system, 4) DAQ system, 5) pressure sensor, 6) control unit, 7) vacuum pump, 8) venting system, 9) air pump, 10) connecting system, 11) plastic membrane, and 12) silencer(Liu et al., 2010)**

## 2.9.2 Large-scale explosion test facility in Australia

The reactor in cylindrical shape, in Figure 6, was built at Newcastle University, Australia. The chamber was built of steel with a length of 30 m and a diameter of 0.5 m. There are several high-resolution pressure transducers, a pyrometer, and a high-speed video camera. Methane and coal dust are used for combustion of fuels and chemical igniters with known energy. The purpose of this study is to test the fire and explosive properties of hybrid fuels in the chemical and process sectors. It also explores the effect of ignition energy and vessel structure on the magnitude of the pressure rise and the propagation of the flame (Ajrash et al., 2017; 2016).

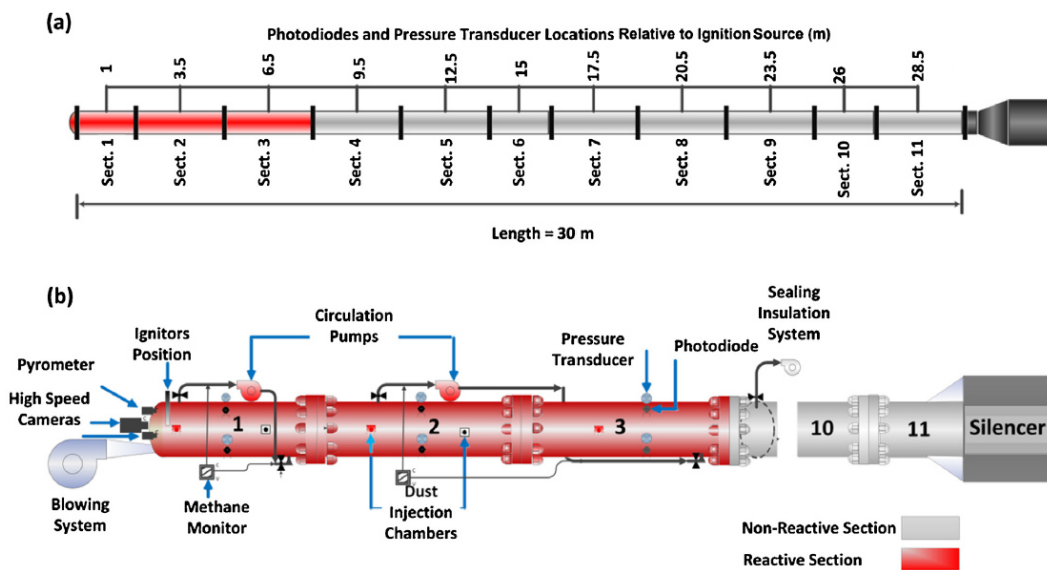


Fig. 4. Components of the LSSD at the University of Newcastle, Australia.

Figure 6: Schematic drawing of the experimental set-up of Australian reactor (Ajrash et al., 2017a)

### 2.9.3 Large-scale explosion test facility in South Africa

Figure 7 shows the 200 m long and 2 m in diameter wide detonation tube in Kloppersbos, South Africa. Figure 8 shows a schematic view of the tube. Initially, the methane/air mixture with a specific concentration is located between a diaphragm and the closed-end of the tube. Two 30 m long areas of coal dust are allotted in the tube. The system is used to detect propagating explosion, to determine the amount of stone dust that has to be applied to the second zone of coal dust in order to suppress the explosion propagation and to test barriers against hybrid explosions (Du Plessis, 2015; Gildfind et. al., 2014).



Figure 7: Experimental setup of the reactor in Kloppersbos, South Africa. Left: aerial view, right: view of the open end

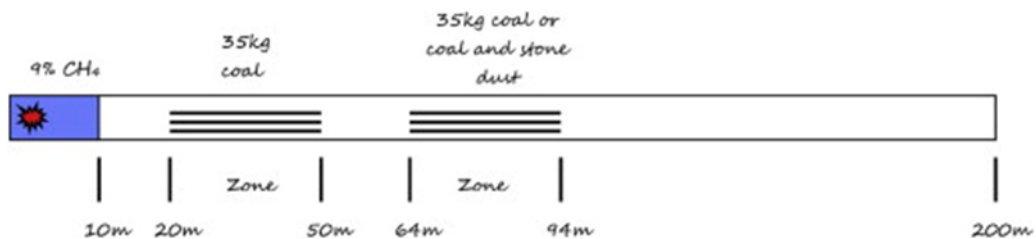


Figure 8: Schematic diagram of the reactor with the length of methane, coal dust and rock dust zones (Du Plessis, 2015)

---

#### 2.9.4 Laboratory-scale and large-scale explosion test facility in the U.S.

---

In the past several years CSM has performed sophisticated CFD modelling and computational work with scaled methane gas explosions in coal mines to predict where explosive methane and air mixtures are likely to form in underground coal mines to establish how methane-air explosions propagate across the mining area and mined gob filled with porous rock. Hereafter, CSM wants to extend its work by conducting explosion tests with coal dust and methane (Fig, 2019; Strebinger, 2019).

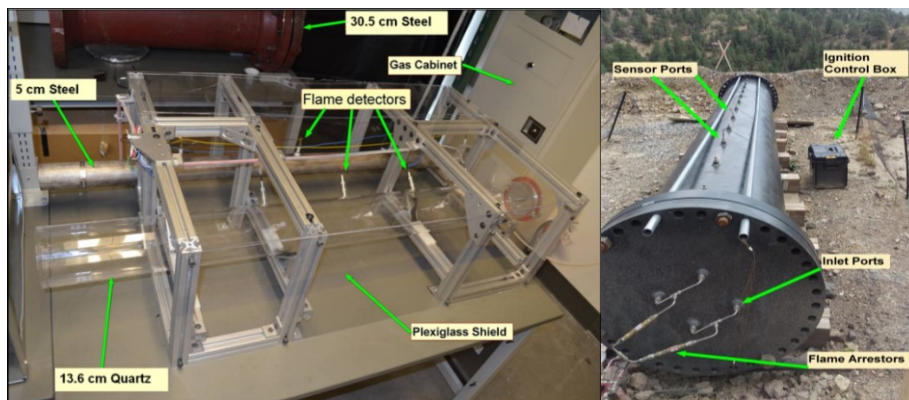


**Figure 9: Experimental setup of reactors at CSM. Left: Quartz reactor for visual methane explosion and steel reactor; Right: View of the large-scale reactor at the Edgar Mine (Fig, 2019; Strebinger, 2019)**

### 3 Experimental setup and investigation of coal dust explosion propagation

An experimental small-scale horizontal steel reactor, which was initially used for methane-air mixture propagation to provide initial investigations about the combustion characteristics in a laboratory scale, is used to perform the methane-air-coal dust tests. All experiments are performed in a controlled environment at standard conditions with 294 K and 83 kPa, the atmospheric pressure in Golden, CO.

#### 3.1 Experimental setup of combustion reactor

In the Figure 10, a schematic replicates the experimental system consisting of industrial-grade compressed methane and zero-grade air, two mass flow controllers (MFC), flame arrestors, a mixing tank, three solenoids, a reactor, four ion sensors, a pressure transducer, a data acquisition system and an exhaust system.

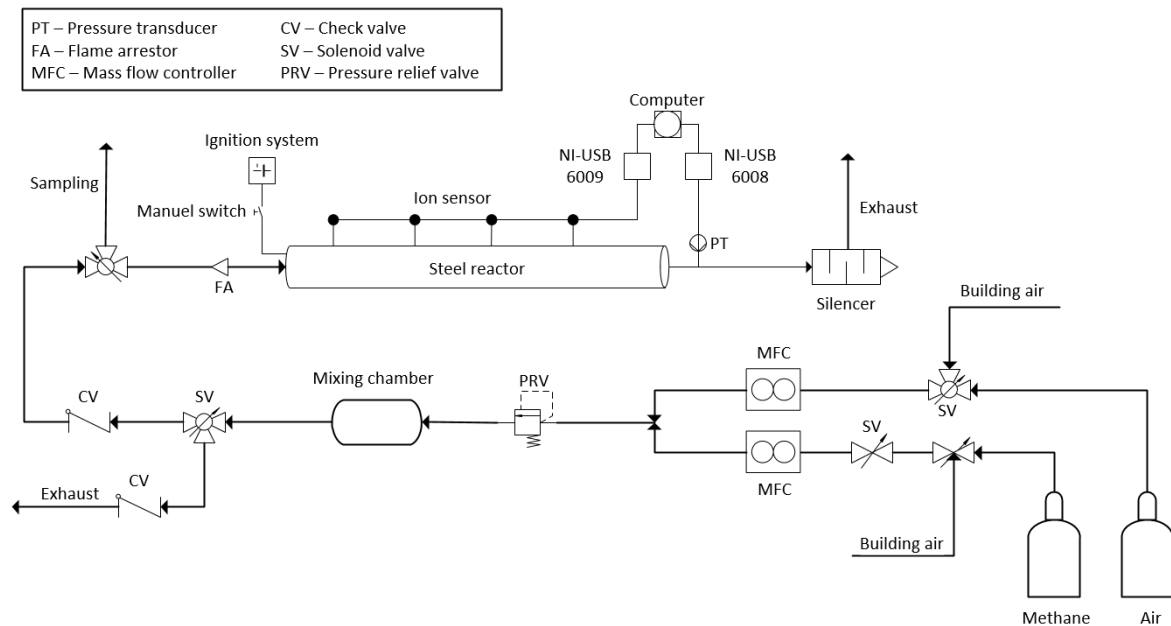


Figure 10: Schematic layout of the experimental steel reactor with all components in the laboratory at CSM

Both the methane and air are supplied from high pressure compressed gas cylinders. Two MFCs control the flow rate. The air flow is controlled by a Bronkhorst EL-FLOW Select (0-50 SLPM) mass flow controller and the CH<sub>4</sub> stream controlled by an Alicat Scientific MC Series mass flow controller (0-5 SLPM). The two gases

are combined in a mixing tank before entering the reactor. A highly porous media which induces turbulences guarantees a homogenous mixture of the two gases prior to entering the reactor. The premixed gases are carried to the reactor. The open end of the reactor is covered with perforated aluminum foil to prevent the backflow of atmospheric air into the reactor. A small hole is made in the foil to purge the remaining air in the reactor by the premixed gases, prevents an increase of the pressure in the reactor.

In order to conduct an experiment, a certain amount of coal dust with 85 % of the particles smaller than  $75\ \mu\text{m}$  ( $d_{85} < 75\ \mu\text{m}$ ) depending on the concentration is placed on a metal plate and slid to the closed end of the reactor. The aluminum foil is folded over the open end. The premixed volume of the two gases equals two to three times the reactor volume flows through the steel reactor for about  $2\ \text{minutes} \pm 5\ \text{s}$  at 30 psi to ensures that the ambient air is completely flushed out. Only the homogenized premix remains in the reactor before the ignition. When the reactor is filled, a waiting time of  $1\ \text{minute} \pm 3\ \text{s}$  assures that the premix can settle for stable conditions. The methane-air mixture is ignited by a capacitive, automotive spark ignition system. The energy of the produced spark is about  $60 \pm 5\ \text{mJ}$ . The propagation of the flame is detected by the four ion sensors, which are connected to a data acquisition (DAQ) device (National Instruments (NI) USB-6008), which measures the signal of the sensors. The pressure wave is measured with the pressure transducer at the open end. This sensor is also connected to the DAQ. After the experiment is completed, the compressed air of the building is flushed through the reactor and lines to purge the remaining combustible products to the exhaust system. The exact procedure to operate the steel reactor is listed as Appendix A.

Safety features are: The gas cylinders are placed in a flammable cabinet, which is connected to the exhaust system of the building. The lines consist of stainless steel and can withstand pressure up to 35 MPa. All the solenoids are connected to the emergency stop button. A two-way valve is used for methane supply, and a three-way valve regulates either air from the pressurized cylinder or purge-air from the building. A pressure relief valve is installed upstream of the mixing tank. The valve opens if the pressure in the lines is higher than 35 kPa. The relieved gases get sucked by the exhaust system. Downstream of the mixing tank, another three-way solenoid valve is installed to either fill the reactor with the premixed gases or purge

the mixture into the flammable cabinet. Two flame arrestors along the reactor filling line and the purge line protect the system in case of accidental combustion. An exhaust system is placed at the open end of the T-junction to extract the exhaust gases and any remaining combustible mixture and a gas leak detector. The three electrical solenoid valves are Senya explosion-proofed and are remotely controlled and connected with the emergency shut down button. The air purge system removes any premixed methane-air mixtures in the lines between the methane cylinder and the reactor. The steel reactor is placed in a 30.5 cm diameter and 1.2 m in length steel tube to protect users in the case of a material failure of the tube or spark plugs. The open end of the T-junction is covered with a filter so that coal dust won't get sucked into the exhaust system. A What-If-Analysis (Appendix B) was developed for the purpose of the experiments if an emergency happens.

---

### **3.1.1 Steel reactor design**

---

The laboratory-scale steel reactor in Figure 11 has a diameter of 6.3 cm and a length of 153 cm, which results in a length/diameter (L/D) ratio of 26. One end is open to the atmosphere, and the other end is closed with an inlet for the ignition system and an inlet for the gas mixture. Along the longitudinal axis there are four ports for the ion sensors. The ports are equally 38 cm apart from each other. The holes are threaded with a diameter of 16 mm, allowing standard automotive spark plugs to be placed into the ports. These spark plugs are used as ion sensors to detect flame propagation. In the center, at the open end, a pressure transducer measures the pressure rise of the propagation. The wall thickness of the tube is 0.6 cm to handle the explosion pressure.

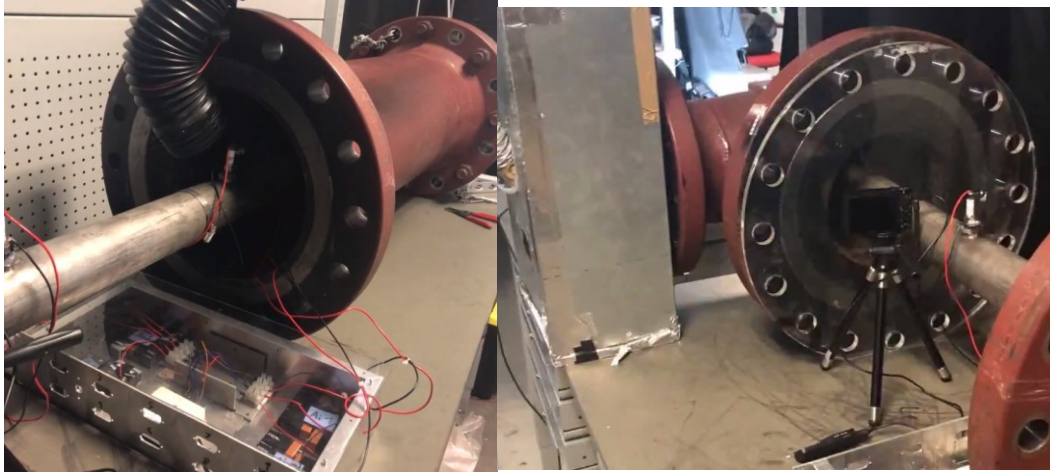


**Figure 11: Left: The 6.3 cm diameter and 153 cm long steel reactor inserted in the 30.5 cm diameter steel reactor with a black hose from the top for the exhaust and the box with the DAQ for the ion sensors; Right: View to the open-end of the steel reactor with high speed imaging and the exhaust box at the open end of the T-junction**

### 3.1.2 Sensor Technology

The test reactor contains two measurement devices: ion sensors to measure the flame speed and pressure transducer two measure the pressure of the blast wave. The flame detector setup was created by using four commercial spark plugs with a voltage source connected to create a potential difference between the electrodes, effectively treating the electrodes as an electrical capacitor. The sensors are in the vertical position of the reactor and placed 38 cm away from each other. The first sensor is placed 5 cm from the spark. Figure 12 shows the circuit for each sensor and the housing for the voltage source, resistors and the DAQ system. The metal box also acts as a faraday cage and reduces noise. Each sensor is in a circuit with its own a resistor.

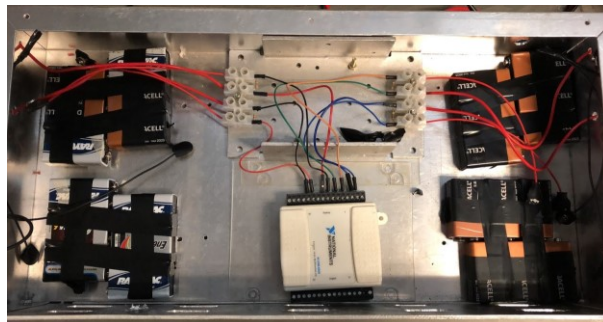
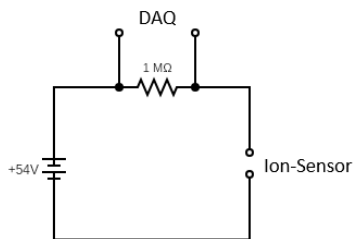


**Figure 12 Left: Schematic of the ion sensor circuit. Value of voltage source is 54 V, value of resistor is 1 MΩ, Right: Metal box with the DAQ system, the four voltage sources for the four sensors and the connection to the DAQ**

When the flame passes near the gap between the electrodes of the ion sensors, the ionized particles create a voltage drop and is being recorded by the DAQ system. The reason for a parallel circuit is to avoid an overlap of the signal; thus, the sample rate of the DAQ device is limited when more channels are connected. The velocity of the flame is calculated by the known distance between the ion sensors and the different times the signals are detected. The Figure 13 shows an example of signal output when the flame is passing the sensors.

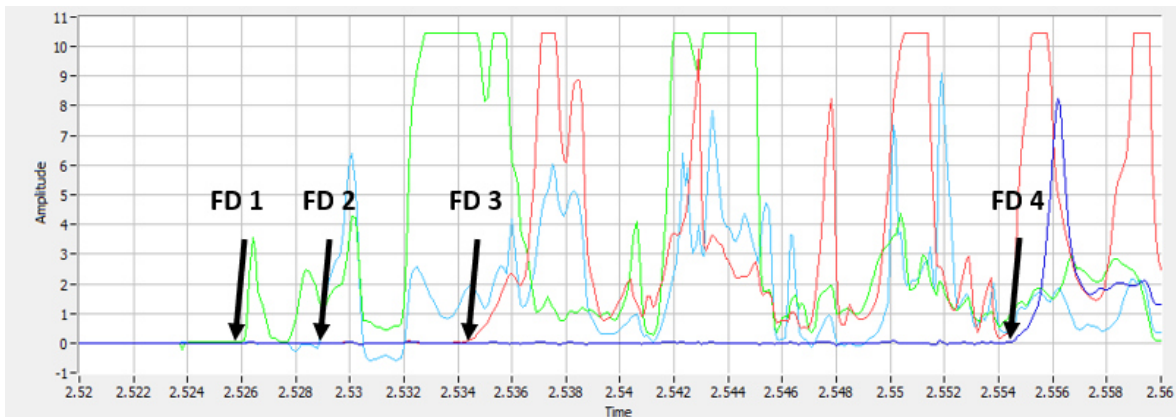


**Figure 13: Typical signal from passing of the flame. In this case the flame was produced by a torch. Each color represents an ion sensor and the first rise, described as flame detection (FD), of each line correspond to the first detection of the flame in voltage as a function of time**

The dynamic pressure of the explosion wave is measured by a piezoelectric pressure transducer. The transducer is located centric at the open end of the steel reactor.

### 3.1.2.1 Ion flame sensors

Different types of circuits for the ion sensors were tested. Figure 14 shows the signal from passing the flame from a normal lighter. The circuit of the ion detectors was connected in parallel using the steel reactor as common ground. The voltage source for this example was about 245 V. The peaks correspond to the detection of the flame as a function of time. The diagram shows that the sensors also detect a signal where the flame did not pass. This effect is noticeable, since the signal of the other sensors also shows a slight deflection as can be observed at the blue line. With increasing flame velocity and temperature, an exact calculation of the flame velocity will not be possible, because the signals of the sensors cannot be separated.

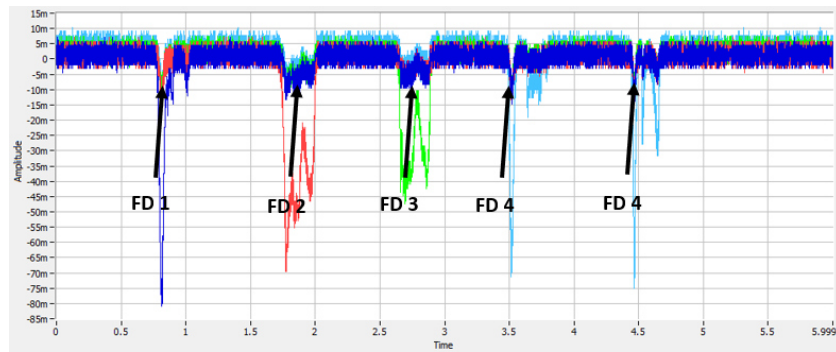


**Figure 14: Signal from passing the flame of a lighter. The voltage peaks are weaker than the peaks from Figure 14.**

### 3.1.3 Coal dust specifications

The coal dust used for the experiments is Pittsburgh seam high volatile bituminous coal. The proximate content and heating value of the fuel was measured by ASTM D3172 and D 1989 and is shown in table 2. The coal dust with the particle size of  $d_{85} < 75\mu\text{m}$  represents the “float” coal dust carried by the airflow of the ventilation system in underground coal mines. The tests were conducted with different coal dust concentrations:  $100\text{ g/m}^3$ ,  $200\text{ g/m}^3$ ,  $416\text{ g/m}^3$ , and  $832\text{ g/m}^3$ . Therefore, the dust was weighted and distributed on a marked zone of a metal plate as shown in Figure 15. This plate was slid into the end of the reactor. The 23 cm zone represents the coal dust zone from the large-scale explosion tube experiments with deposited coal dust from Kloppersbos, South Africa. Figure 15 also shows the preparation of the dispersed coal dust on the metal plate with a concentration of  $432\text{ g/cm}^3$ . The amount of coal dust used in the test is 2 g relative to the volume of the steel tube.

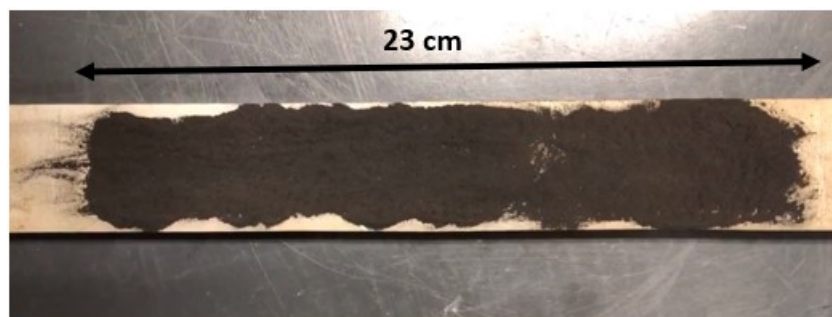


**Figure 15: Deposited coal dust on the metal plate**

**Table 1: Specification of the Pittsburgh coal dust**

<b>Values</b>	<b>Pittsburgh high-volatile bituminous coal</b>
Moisture [%]	1
Volatile matter [%]	37
Fixed carbon [%]	56
Ash [%]	6
Heating value [kJ/kg]	32,322

---

### **3.1.4 Ignition system**

The schematic in Figure 16 shows the single spark ignition system, which consists of a commercial 12 V auto battery, 30 A fuse, resistor, 2  $\mu$ F capacitor, ignition coil, and a manual switch. The spark is produced by flipping the manual flip twice with a short delay. With the first flip, the current is being stored in the capacitor, and the second flip of the switch disconnects the battery current, and the magnetic field breakdown occurs between the ignition coil and the capacitor. The coil increases the voltage across the two electrodes of the spark, which produces the spark. Referred to the thesis of Strebinger (2019) and Fig (2018), the ignition system provides an energy of approximately  $60 \pm 5$  mJ. The system guarantees constant energy of the initial ignition to provide better-quantified results.

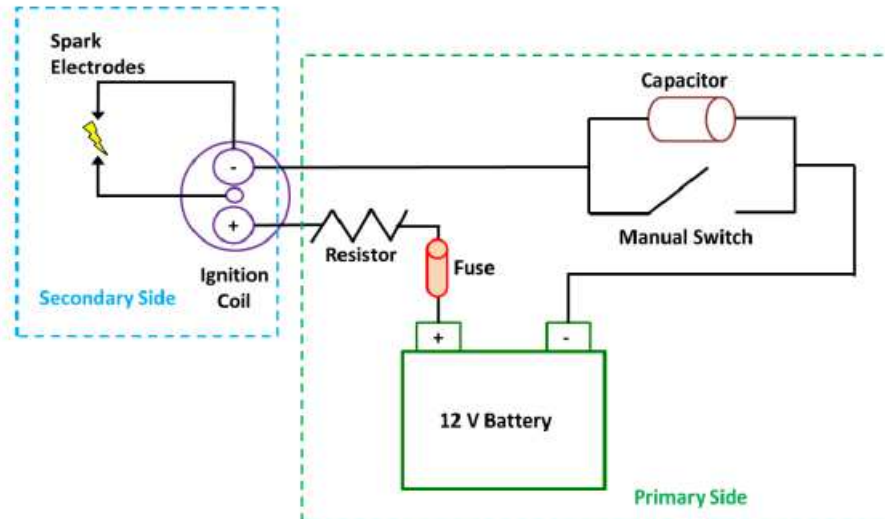


Figure 16: Schematic of the spark ignition system (Strebinger, 2019)

Due to the high current (5 A) of the system, several safety features for a safe handling were installed. The wires are always disconnected from the battery, the ignition coil, and the capacitor after the experiment sessions.

### 3.2 Conduction of the coal dust explosion tests in the steel reactor

Table 2: Summary of all experiments carried out and the mean flame front propagation velocities ( $\bar{V}$ ) and mean standard deviations ( $\overline{SD}$ ) of each series of test

Test index	Unit	1	2	3	4	5	6	7	9	10	11
Rock/ coal dust				Rock	Coal	Coal	Coal	Rock	Coal	Coal	Coal
Dep/ disp				dep	dep	dep	dep	disp	disp	disp	disp
Amount of dust	g	0	0	2	0.5	2	4	0.5	0.5	0.5	1
# of tests	#	5	4	3	4	4	2	2	4	4	4
$\bar{V}_{sp-1}$	m/s	3.2	4.1	4	4.2	4.4	4	3.9	4	4.1	3.3
$\bar{V}_{1-2}$	m/s	9.4	12	12	11	11	12	9.2	10	11	9.8
$\bar{V}_{2-3}$	m/s	22	45	43	41	39	39	19	28	34	31
$\bar{V}_{3-4}$	m/s	36	70	48	51	39	34	46	36	35	19
$\overline{SD}_{sp-1}$	m/s	0.69	0.33	0.2	0.18	0.79	0.012	0.027	0.22	0.29	0.23
$\overline{SD}_{1-2}$	m/s	2.7	0.47	0.37	0.63	0.71	0.38	0.18	1	1.9	0.7
$\overline{SD}_{2-3}$	m/s	6.9	2.5	4.4	5.1	5.8	0.12	5.9	2.5	7.5	3.9
$\overline{SD}_{3-4}$	m/s	7.3	9.8	6.7	7.6	2.5	4.8	10	4.2	3.7	1.1

### 3.2.1 Results for methane-air explosions

Initial experiments were performed with a stoichiometric mixture of methane and air to check sensor and system functions. The CH<sub>4</sub>-MFC was set to 1 SLPM, and the air-MFM was set to ~ 11.2 SLPM to assure a stoichiometric mixture. After 2 min of filling time and 1 min of settling time, the combustible mixture was ignited. The ion sensors detected the flame with a readable signal to determine the flame velocity. Figure 17 shows a typical graph of the sensors when the flame propagates through the reactor. Each color of the line represents a different sensor. The software “Scout” from National Instruments was used to determine the time when the flame passed a sensor. Knowing the distance between sensors, researchers calculated the flame speed between sensors.

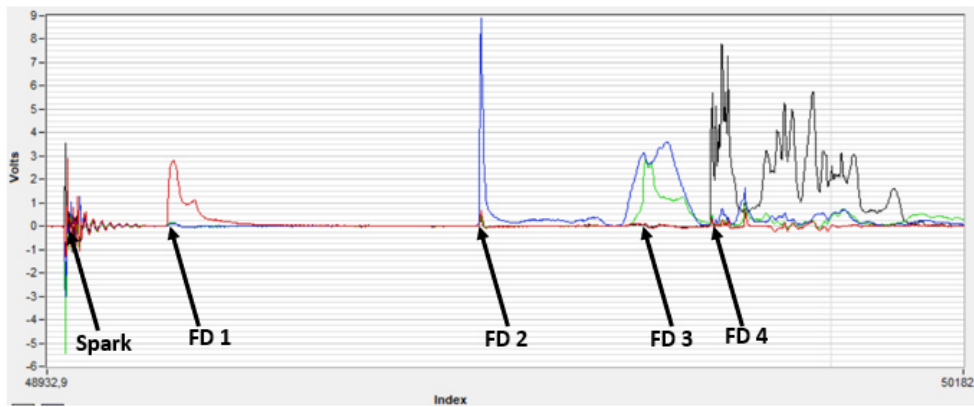
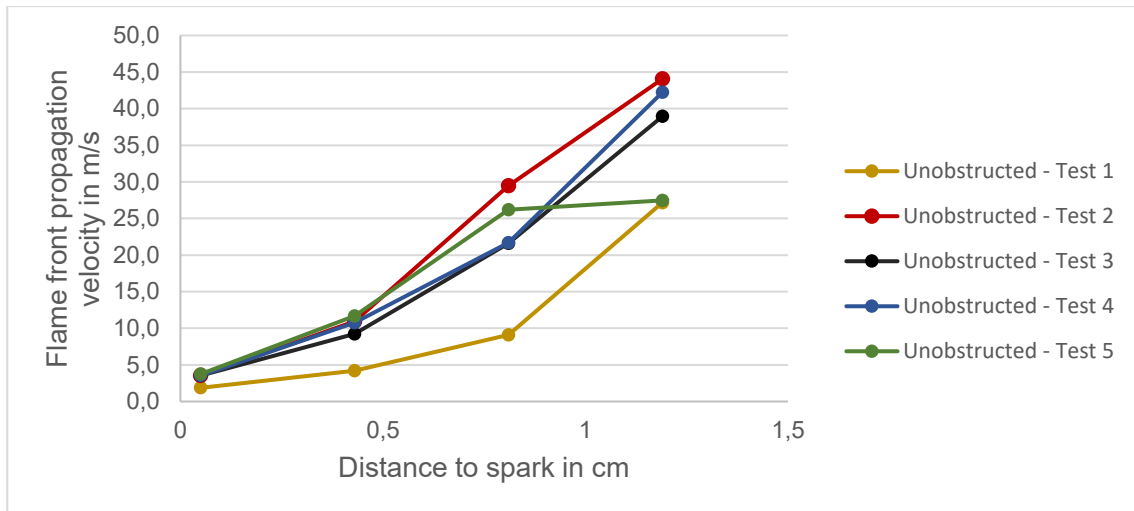


Figure 17: Output from the ion sensors with Scout. X-axis is a function of the Index which refers to the numbers of samples taken with a specific sample rate (Hz)

Figure 18 shows results of the first set of experiments with a stoichiometric mixture of methane and air. In total, five tests were conducted. The filling time and the settling time varied for two of the tests with the empty reactor. This has the effect that the flame velocity tends to be faster when the mixture is ignited after a shorter settling time, due to some gas leakage through the hole of the aluminium foil. A maximum velocity of 44 m/s was measured between the 3rd sensor and the 4th sensor. After ignition, the velocity increased from 3.2 m/s to an average velocity of 36 m/s in the last measuring sector ( $\bar{v}_{3,4}$ ). Due to the variation of the settling times after filling, the standard deviation was 26 %.



**Figure 18: Impact of stoichiometric mixture on methane flame front propagation velocity; mixture volume is within  $\pm 0.3\%$ ;  $SD_{\text{mean}} = 26\%$ .**

Figure 29 shows a mainly blue color of the flame of the methane-air mixture due to stoichiometric combustion. The picture was taken at the open end of the reactor.



**Figure 19: Image of a stoichiometric flame leaving the open-end of the steel reactor**

### 3.2.2 Results of the obstructed reactor with the metal plate

The next set of experiments was conducted with the obstructed reactor in a stoichiometric methane-air medium. This was necessary because any obstacle in the reactor causes turbulences. These, in turn, cause higher flame velocity. The metal plate has nearly the same length ( $L = 147$  cm) as the reactor for easier and safer placing in the steel tube. Referred to former experiments conducted by Fig (2019) and Strebinger (2019), the flame velocity increases significantly when an obstacle is placed in the reactor.

Therefore, experiments are also performed only with the steel plate to see how the velocity varies. Five tests were carried out to obtain an illustrative result shown in Figure 20. The results of the flame velocity showed an average increase of 64 % over the entire length of the reactor. At the end of the reactor, the average speed was 70 m/s. This is almost two times faster than the velocity in the unobstructed reactor (36 m/s). The highest velocity measured between the 3<sup>rd</sup> and 4<sup>th</sup> sensor was 83 m/s, with the lowest 59 m/s. The deviation can again be related to the fact that any slight change in the gas mixture composition changes the explosive nature of the mixture, and this, in turn, affects the flame velocity. Furthermore, the position and inclination of the metal plate can change the turbulence in different ways. The filling and settling time were kept within  $\pm 5$  s in these tests, which also has an effect on the deviations.

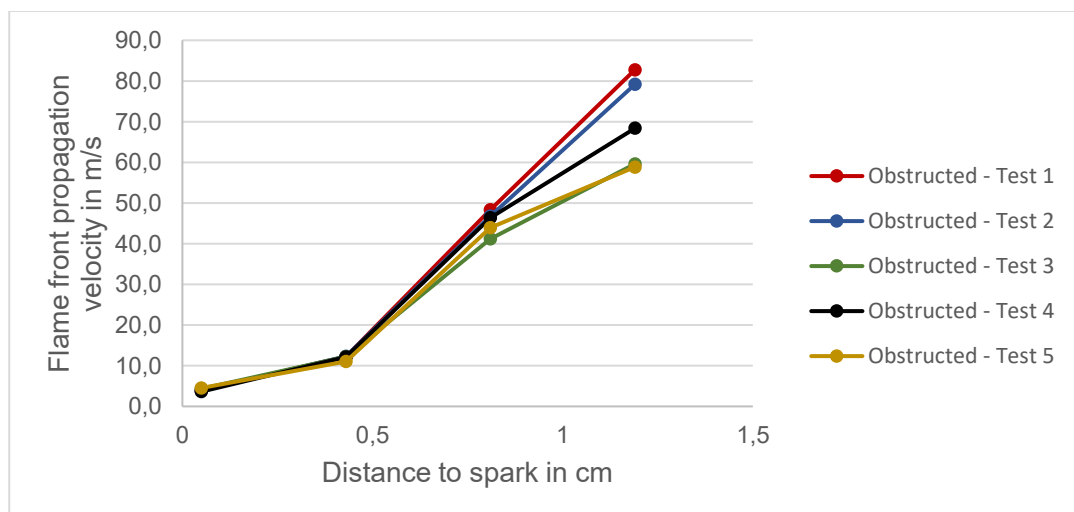


**Figure 20: Impact of stoichiometric mixture on methane flame front propagation velocity; mixture volume is within  $\pm 0.3$  %;  $SD_{\text{mean}} = 7.9$  %**

---

### 3.2.3 Impact of the deposited rock dust

---

A series of tests was performed prior to testing coal dust to ensure that the rock dust is highly agitated and that the exhaust air system was capable of capturing all dust. The ventilation system was modified slightly so that no dust entered the laboratory air. This series of tests was also used to study how the rock dust influences the flame.

The rock dust was distributed by hand in the same way as the coal dust on the plate in the predefined zone. The plate was placed in the steel reactor. The concentration of the gas mixture and the filling and settling time remained unchanged. The amount of rock dust was 2 g. This corresponds to a concentration of  $\sim 420 \text{ g/m}^3$ . The rock dust is limestone from Germany. Three tests were carried out with this concentration. The results are shown in Figure 21. The result shows also that the rock dust has an effect that decelerates the flame velocity. However, this effect only occurs between the 3<sup>rd</sup> and 4<sup>th</sup> sensor. The mean velocity between the last two sensors was 48 m/s. This corresponds to a reduction of 31 % (70 m/s for speed only with the steel plate in the reactor). The mean value of the total change in the reduction of flame velocity was about 10 %. These phenomena can be attributed to the fact that the rock dust that is dispersed by the shockwave acts as an absorption medium and contains the heat of the flame. If a sufficiently large amount of rock dust is dispersed, the explosion may be completely suppressed. However, it was observed in this case that just a very small portion of the amount was dispersed and that the heat sink effect was relatively low. On average, the standard deviation was 8.1 %. This again is due to the deviations of the filling and settling times, the gas mixture concentration, the distribution of the rock dust, and the amount of rock dust. The highest standard deviation between the 4<sup>th</sup> and 3<sup>rd</sup> sensors was 14 %.

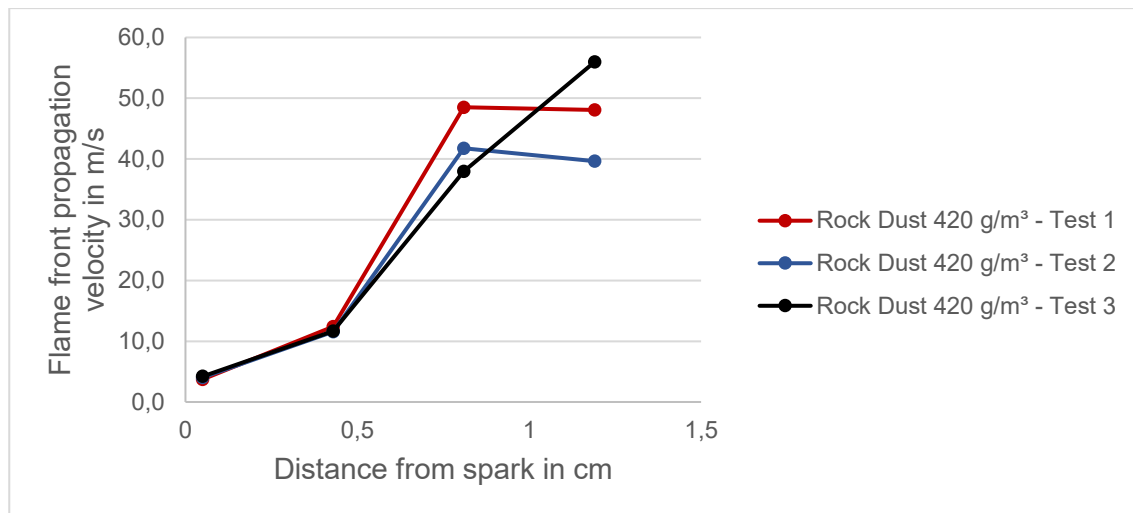


**Figure 21: Impact of stoichiometric mixture on flame front propagation velocity; mixture volume is within  $\pm 0.3\%$ ;  $SD_{\text{mean}} = 8.1\%$**

### 3.2.4 Impact of the deposited coal dust

The following tests were conducted with coal dust of different coal dust concentrations placed on the metal plate. The beginning of the coal dust zone was 20 cm away from the spark. The dust was placed by hand on the plate in a predefined zone and evenly distributed with a brush. The length of the coal dust zone is 23 cm. Filling and settling time and the composition of the methane-air mixture were not changed. The concentrations of the dust were 100, 420, and 830 g/m<sup>3</sup>, converted to the related reactor volume. This results in quantities of 0.5, 2, and 4 g. The table 3 summarizes the number of tests performed per concentration.

**Table 3: Overview of conducted test in steel reactor with metal plate and dust**

Rock/ coal dust	Coal	Coal	Coal
Mass of dust (g)	0.5	2	4
Dust concentration (g/m <sup>3</sup> )	100	420	830
Number of tests	4	4	2

### 3.2.4.1 Coal dust concentration of 100 g/m<sup>3</sup>

The concentration of 100 g/m<sup>3</sup> of the coal dust is the lower limit of explosion according to Michelis (1998) and Stephan (1998) and should have the least influence on the velocity of flames according to the literature. Figure 22 shows the velocity of each test conducted. The highest average velocity measured was 51 m/s, which is 27 % lower than the velocity with the metal plate (70 m/s) and 5.9 % higher than the velocity with rock dust (50 m/s). The standard deviation was 9.3 % on average. This is again dependent on the deviation of the time of filling / settling, the gas mixture concentration, the inclination of the metal plate and its position, the exact weight of the coal dust, the distribution of the coal dust and the loss of dust particles while handling.

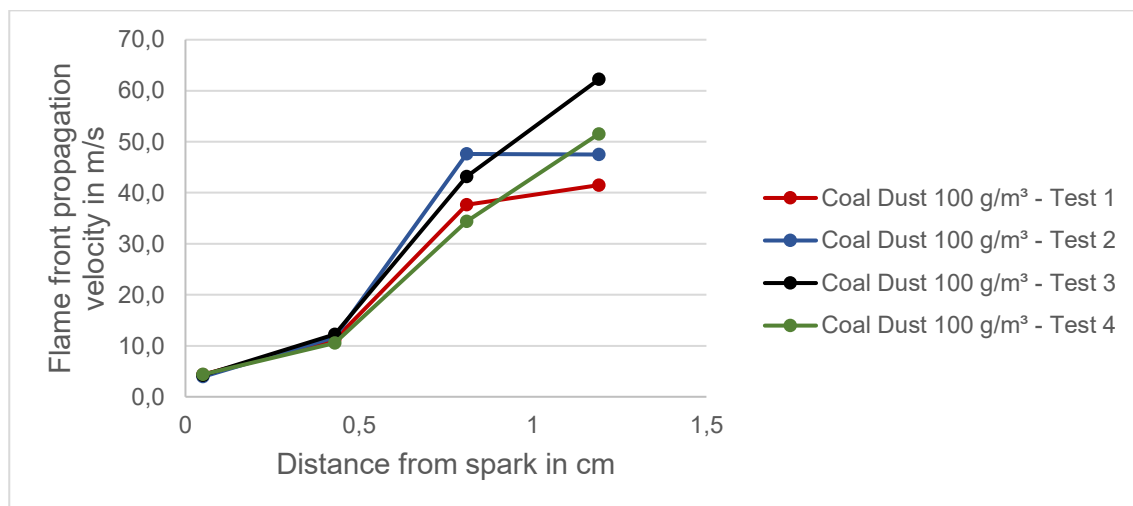
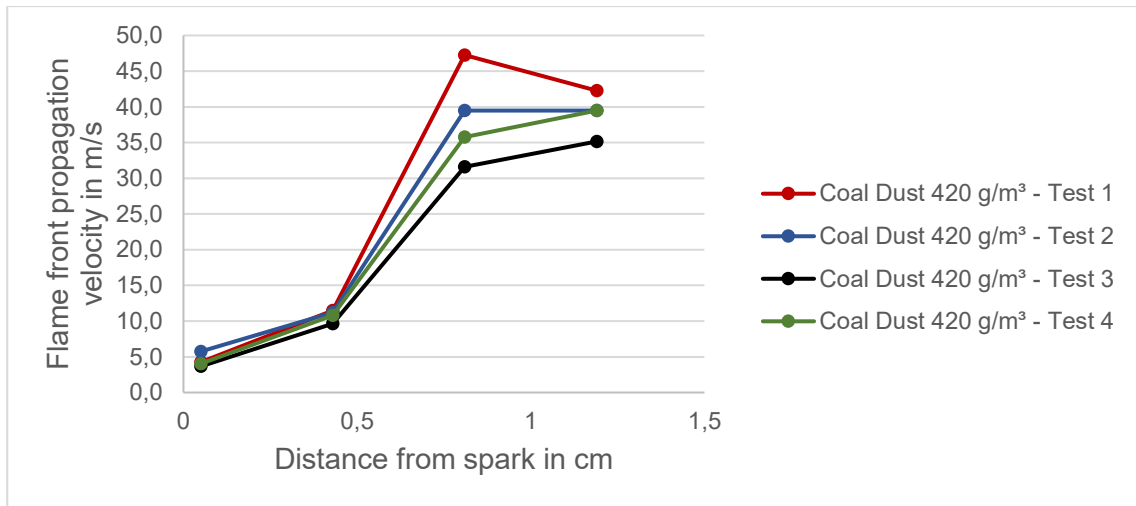


Figure 22: Impact of stoichiometric mixture on flame front propagation velocity; mixture volume is within  $\pm 0.3\%$ ;  $SD_{\text{mean}} = 9.3\%$

### 3.2.4.2 Coal dust concentration of 420 g/m<sup>3</sup>

In this series of experiments, four tests were performed. Figure 23 refers to flame velocity between the measuring sensors for each test. The standard deviation is 12% based on the variations between tests as described in the previous chapter. The average maximum velocity measured is between 3<sup>rd</sup> and 4<sup>th</sup> and is 39 m/s. Differences can also be seen in these tests, particularly between the last two ion sensors. Here, the velocity is 23 % lower than in the 100 g/m<sup>3</sup> carbon dust test.



**Figure 23: Impact of stoichiometric mixture on flame front propagation velocity; mixture volume is within  $\pm 0.3\%$ ;  $SD_{\text{mean}} = 12\%$**

### 3.2.4.3 Coal dust concentration of 830 g/m<sup>3</sup>

A total of two tests were carried out with this coal dust concentration. Due to the small number of tests, this does not have much informative value, but it reflects a trend, and with a standard deviation of 4.5 % relative to all measured values, it is one of the lowest of all test series carried out. It should be emphasized that at this concentration, there is a reduction in flame velocity between the 3<sup>rd</sup> and 4<sup>th</sup> measuring points. The velocity between the 2<sup>nd</sup> and 3<sup>rd</sup> sensors is 39 m/s and decreases to 34 m/s. The flame velocity behaves in a similar way as in the other tests.

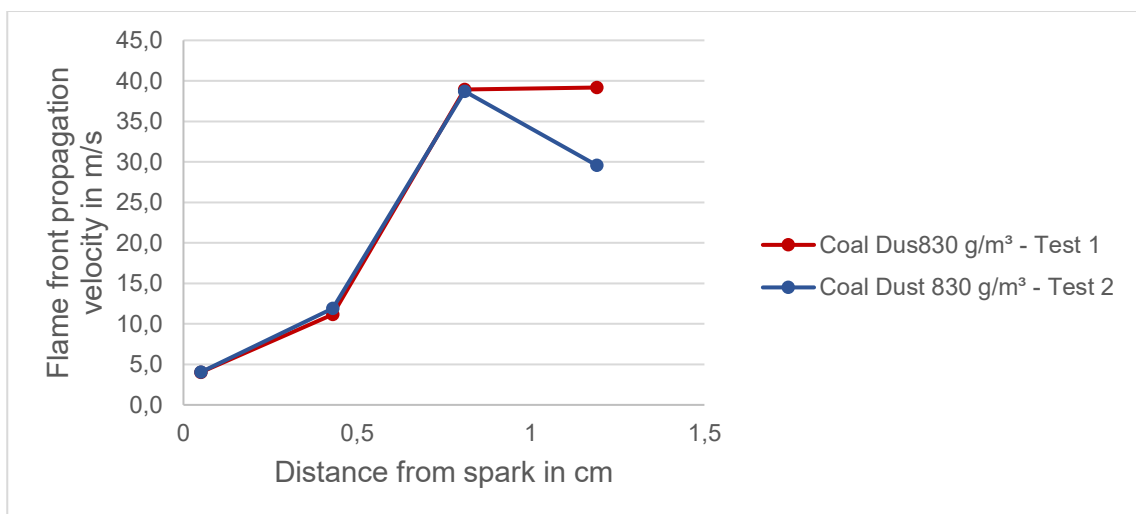


**Figure 24: Impact of stoichiometric mixture on flame front propagation velocity; mixture volume is within  $\pm 0.3\%$ ;  $SD_{\text{mean}} = 4.5\%$**

### 3.2.5 Effect of deposited coal dust with different concentrations

In the tests with coal dust deposited on the metal plate, the flame speed was also reduced as in the test with rock dust. The result is different from that according to the literature, as the addition of a certain amount of coal dust increases the flame front velocity. However, all these experiments were tested in vessels with pre-dispersed coal dust and in longer tubes with a higher L/D ratio. A much stronger initiator was also used in these tests. Ajrash et al. (2016) have used an ignition source of 1 kJ to 10 kJ in their tests. The ignition source of the laboratory-scaled tests is 60 mJ.

The reduction of the flame speed can also be explained by the fact that the dispersed coal dust particles absorb the heat, and the energy is too less to evolve the gaseous substances of the volatile matter of the coal dust particles, which act as fuel for the explosion. The absorption has the effect of reducing the temperature of the flame and slowing down the flame velocity. With an L/D ratio of 26, the reactor is relatively small. For comparison, the reactor in Australia has an L/D ratio of 60 (Ajrash et al., 2017a, 2017b, 2016). The Kloppersbos reactor in South Africa with an L/D ratio of 100 is almost twice as large as that in Australia. Du Plessis (2015) and Liu et al. (2010) tested pulverized coal in a reactor with an L/D ratio of 140. A shorter reactor length means that the coal dust particles may not be exposed to the flame for long enough and little to no energy is released by combustion of volatile matter so the dust explosion may not propagate.

**Table 4: Overview of all tests carried with the metal plate inside the reactor.**

Rock/ coal dust		No Dust	Rock	Coal	Coal	Coal
<b>Amount of dust</b>	<b>g</b>	0	2	0,5	2	4
<b>Number of tests</b>	<b>#</b>	4	3	4	4	2
$\bar{V}_{sp-1}$	<b>m/s</b>	4.1	4.0	4.2	4.4	4.0
$\bar{V}_{1-2}$	<b>m/s</b>	12	12	11	11	12
$\bar{V}_{2-3}$	<b>m/s</b>	45	43	41	39	39
$\bar{V}_{3-4}$	<b>m/s</b>	70	48	51	39	34
$\bar{SD}_{sp-1}$	<b>m/s</b>	0.33	0.20	0.18	0.79	0.012
$\bar{SD}_{1-2}$	<b>m/s</b>	0.47	0.37	0.63	0.71	0.38
$\bar{SD}_{2-3}$	<b>m/s</b>	2.5	4.4	5.1	5.8	0.12
$\bar{SD}_{3-4}$	<b>m/s</b>	9.8	6.7	7.6	2.5	4.8

The results in Figure 25 are the mean velocities plotted from table 4. The test series with the lowest concentration (100 g/m<sup>3</sup>) still had the highest flame speed, because a lower amount of coarser coal dust particles was available for absorption. Furthermore, it was observed that in all tests, the color of the flame was yellow. This effect is an indicator of blackbody radiation. This phenomenon occurs when glowing or burning soot particles are present. The black body radiation can be observed at all concentrations.

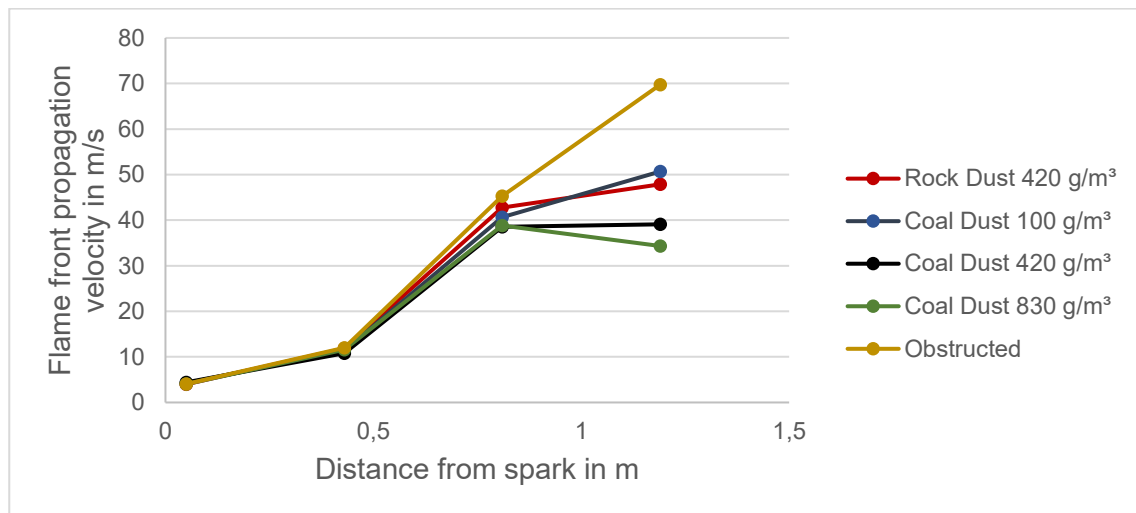


**Figure 25: Average flame front propagation velocity of all tests carried out with no dust and deposited coal and rock dust; Operating conditions:  $294 \pm 1$  K,  $83 \pm 1$  kPa and  $E_{ign}=60 \pm 5$  mJ**

Figure 26 shows the comparison of the tests with the methane-air medium without the metal plate (unobstructed), methane-air medium with the metal plate (obstructed) and the deposited coal dust with the concentrations of 100, 420 and 830 g/m<sup>3</sup>. It can be observed that the propagation velocity of the flame between the 3<sup>rd</sup> and 4<sup>th</sup> sensor at a concentration of 830 g/m<sup>3</sup> is lower than the propagation velocity without metal plate. The highest velocity occurs in the experiment with the metal plate only.

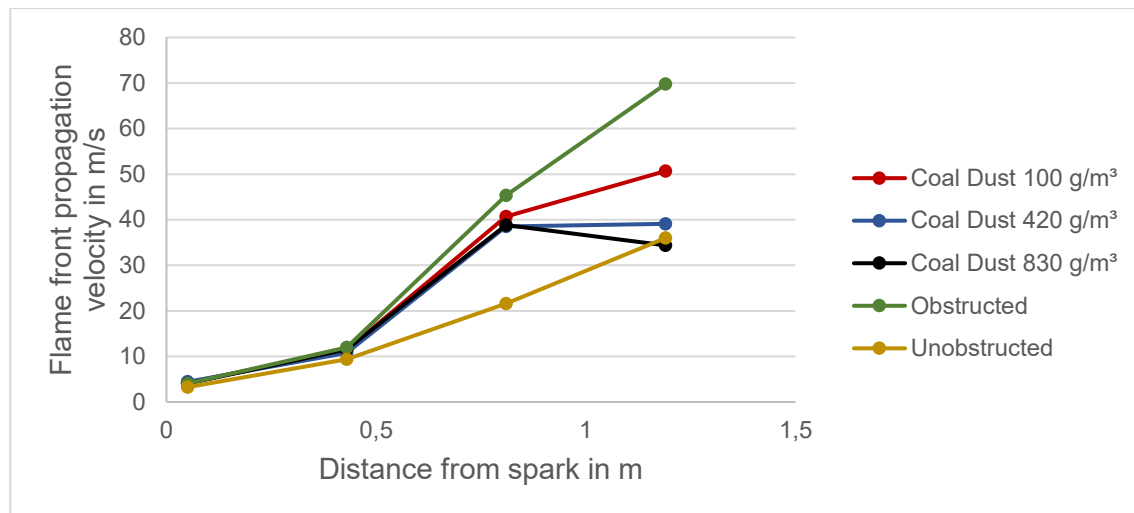


**Figure 26: Average flame front propagation velocity of all tests carried out with no coal dust and deposited coal; Operating conditions:  $294 \pm 1$  K,  $83 \pm 1$  kPa and  $E_{ign}=60 \pm 5$  mJ**

### 3.2.6 Impact of the dispersed coal dust

After the tests with deposited coal dust and the corresponding results, tests with dispersed coal dust shortly before ignition were carried out to see whether the effect can also be observed with the dispersed coal dust or whether there is an increase in the flame velocity, as the amount of finer coal dust particles is higher due to the pre-dispersion. The setup was slightly modified for these experiments. With the help of the building air at a pressure of 20 psi and an air volume of approx. 380 cm<sup>3</sup> the pulverized coal was injected from the open end of the steel reactor about 1 s before the ignition of the methane-air mixture. The effects of rock dust and coal dust on the flame velocity were investigated. The methane concentration was 9.5 %, as in all experiments. The filling time remained constant at 2 min  $\pm$  5 s, and the settling time was kept constant at 1 min  $\pm$  3 s. The reactor was cleaned after each test with a normal industrial vacuum cleaner to remove coal dust particles that did not participate in the reaction.

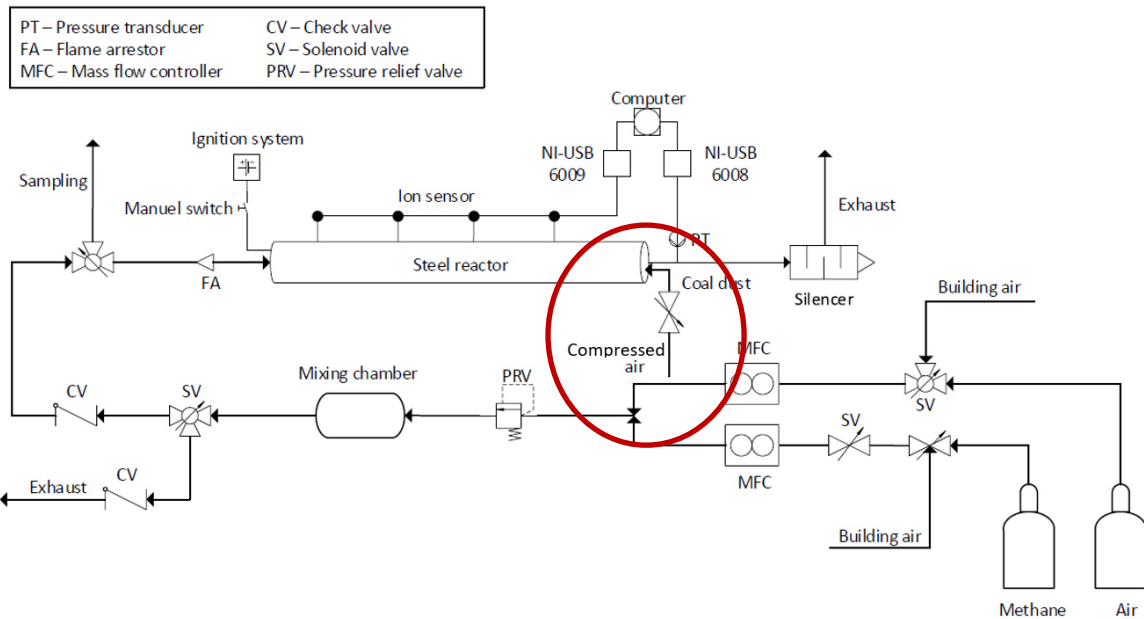


**Figure 27: Modified schematic layout of the experimental steel reactor with all components to pre-disperse the coal dust into the reactor. The red circle indicates the line and valve to inject the dust**

### 3.2.6.1 Impact of dispersed rock dust without metal plate

The first experiments were tested with rock dust in an unobstructed reactor. This involved injecting 0.50 g (100 g/m<sup>3</sup>) of the rock dust into the tube. Two tests were carried out with this amount. The standard deviation is ~14 % on average, but larger deviations were calculated on the last two measuring sections. The difference in flame velocity between the two tests is 20 m/s between the 3<sup>rd</sup> and 4<sup>th</sup> sensors and 10 m/s between the 2<sup>nd</sup> and 3<sup>rd</sup> sensors. Due to the high deviations and a low number of tests, a quantitative conclusion is not possible.

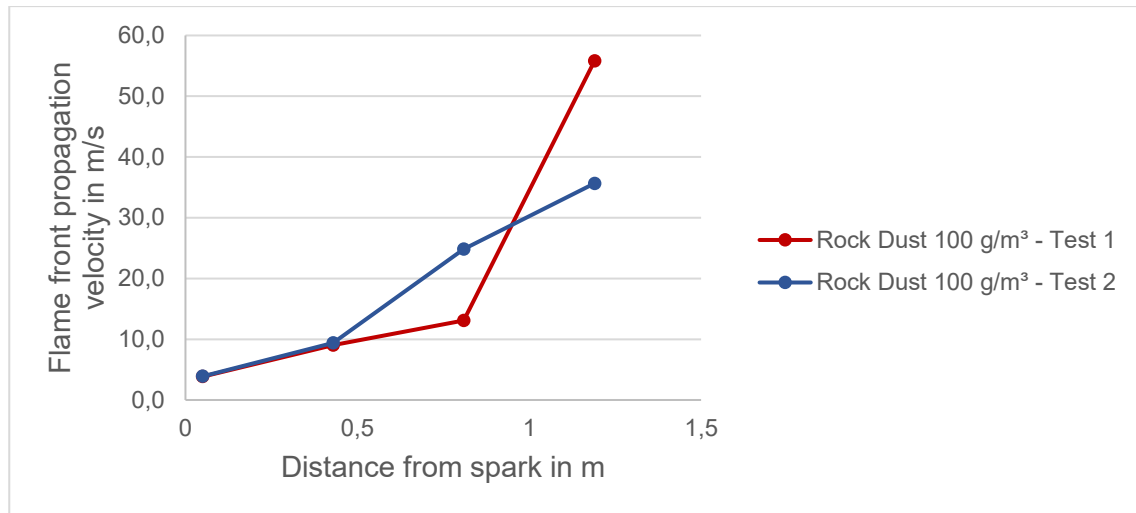


**Figure 28: Impact of stoichiometric mixture on flame front propagation velocity; mixture volume is within  $\pm 0.3\%$ ;  $SD_{\text{mean}} = 13.9\%$**

### 3.2.6.2 Coal dust concentration of $100 \text{ g/m}^3$ without metal plate

In total, four tests were carried out with a concentration of  $100 \text{ g/m}^3$ , which in turn corresponds to  $0.5 \text{ g}$  of coal dust. The mean value of the standard deviation for this test series was  $9.0\%$ . The end velocity of the flame, which could be measured was  $36 \text{ m/s}$  on average for the four tests. This value is  $1\%$  higher than the value with the unobstructed reactor ( $36 \text{ m/s}$ ). The velocity between the 2<sup>nd</sup> and 3<sup>rd</sup> sensors ( $26 \text{ m/s}$ ) is also higher than the velocity in this section with the unobstructed reactor ( $22 \text{ m/s}$ ). It can be observed that the finest coal dust particles have an influence on the flame velocity and release volatile gases, which act as an energy source for the explosion. Due to the pre dispersion of the coal dust, the highest concentration is found in the area where the higher velocities were measured. The velocity close to the spark was unchanged compared to the velocity with the unobstructed reactor.

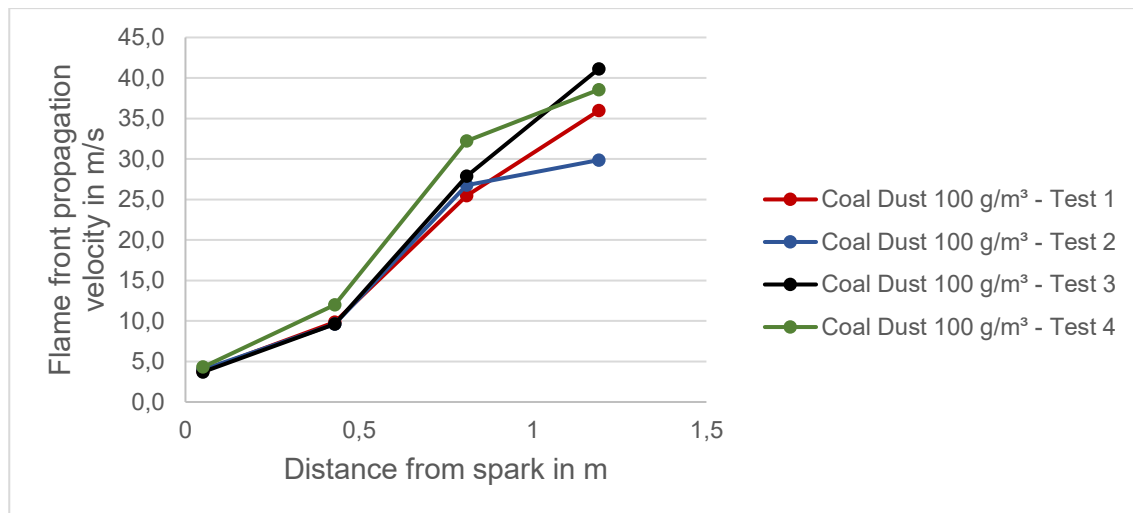


**Figure 29: Impact of stoichiometric mixture on flame front propagation velocity; mixture volume is within  $\pm 0.3\%$ ;  $SD_{mean} = 9.0\%$**

### 3.2.6.3 Coal dust concentration of $100\text{ g/m}^3$ with a metal plate

This experiment gives a direct comparison between the experiments with the metal plate and the coal dust placed on it, since more turbulences are created with the plate and higher velocities of the flame are expected. Thus, a reference can be made to the effect of the flame velocity. In this case, the metal plate was placed in the steel reactor during each experiment and cleaned after each test. A total of four tests were performed with this concentration. The standard deviation was  $14\%$ , with the highest deviation between the 2<sup>nd</sup> and 3<sup>rd</sup> sensors being  $22\%$ . The metal plate could be an obstacle to a consistent distribution of the coal dust. The highest velocity was measured between the 3<sup>rd</sup> and 4<sup>th</sup> ion sensors at  $35\text{ m/s}$ . However, this is only  $1.2\text{ m/s}$  higher than the speed between the 2<sup>nd</sup> and 3<sup>rd</sup> sensors. The big difference between the test with the metal plate should be emphasized. The average value of the velocity of the flame between the 3<sup>rd</sup> and 4<sup>th</sup> sensor is  $70\text{ m/s}$ . This is a reduction of more than twice the value. The metal plate also reduces the volume by dispersing the carbon dust, which in turn leads to an increase in the carbon dust concentration. This phenomenon has been observed in the tests with the deposited carbon dust. In these experiments the flame velocity was also reduced with increasing concentration.

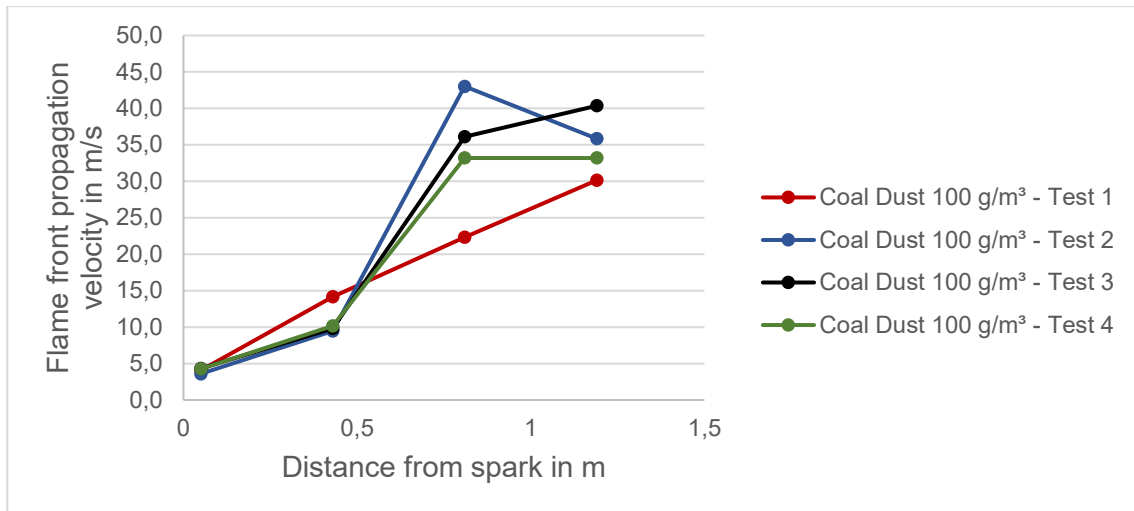


**Figure 30: Impact of stoichiometric mixture on flame front propagation velocity; mixture volume is within  $\pm 0.3\%$ ;  $SD_{mean} = 14.4\%$**

### 3.2.6.4 Coal dust concentration of 200 g/m³ with the metal plate

The last test series was carried out with a concentration of 200 g/m³ in order to be able to make a more precise statement about how the flame velocity behaves when the coal dust concentration is increased for pre-injected experiments. Four tests were conducted. The mean value of the standard deviation of all measured flame velocities is 8.1 %. Here again, the effect was observed that the velocity is throttled at the last measuring zone. Between the 3<sup>rd</sup> and 4<sup>th</sup> sensors, the average speed is 19 m/s, which is 42 % lower than the average speed at a carbon concentration of 100 g/m³.

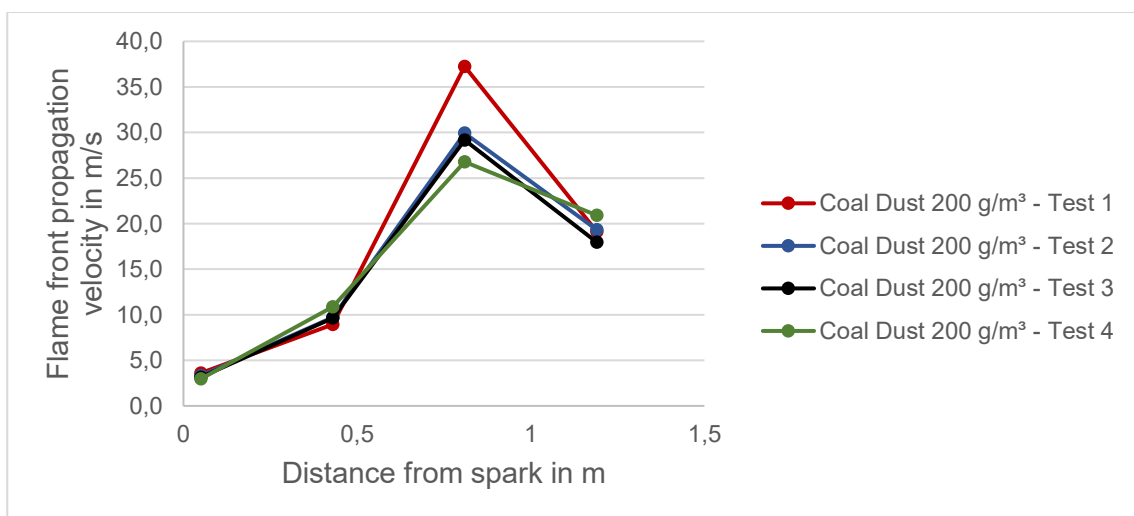


**Figure 31: Impact of stoichiometric mixture on flame front propagation velocity; mixture volume is within  $\pm 0.3\%$ ;  $SD_{mean} = 8.1\%$**

### 3.2.7 Effect of pre-dispersed dust

The test series with the pre-injected pulverized coal dust has confirmed a trend. As observed in the tests with coal dust deposited on the metal plate, the injected coal dust has a negative influence on the flame velocity. The higher the amount of coal dust injected, the lower the flame speed. It is noticeable that the deposited coal dust with a quantity of 0.5 g has a higher average flame velocity (51 m/s) between the 3<sup>rd</sup> and 4<sup>th</sup> sensor compared to the test with 0.5 g dispersed coal dust and a quantity of (33 m/s). This is because the dispersion before ignition provides a greater proportion of coal dust particles for energy absorption than the deposited dust. This effect is even intensified with a higher concentration (200 g/m<sup>3</sup>) since the average velocity in the last measuring sector is only 19 m/s. Figure 32 shows these results. The drop of the velocity between the 3<sup>rd</sup> and 4<sup>th</sup> sensor can be explained by the fact that the more coal dust is added, the lower the concentration of the methane-air mixture. By reducing the concentration of the gas mixture, the flame velocity and the temperature decrease, which affects the energy required to release the volatile gases. Else the more particles of coal, the higher the absorption of the heat.

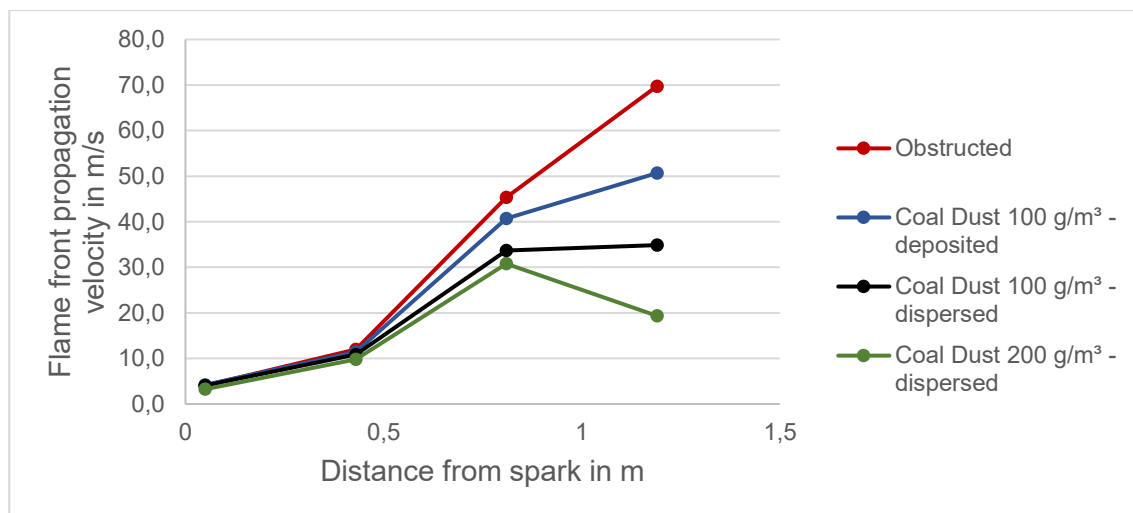


Figure 32: Comparison of the mean flame front propagation velocity for test with the metal plate in the steel reactor

The differences in flame velocities between the spark and the first sensor and between the 1<sup>st</sup> and the 2<sup>nd</sup> sensor are relatively minimal since the coal dust in this area does not yet have any influence on the flame. Only between the 2<sup>nd</sup> and the 3<sup>rd</sup> sensor, the reduction of the speed by the coal dust becomes noticeable.

Figure 33 shows images from high-speed recordings with strong blackbody radiation and a large flame at the end of the reactor than in the experiments with the placed pulverized coal, which can be described by the higher participation of fine coal dust particles in the reaction. By injection, a much higher percentage of the finest particles is exposed to the flames.



**Figure 33: Images of the experiment with 0.5 g of pre-dispersed coal dust before ignition. Flame was filmed from the side of the open end of the steel reactor.**

## 4 Experimental reactor with rectangular cross-section

Researchers also developed a reactor with rectangular cross section to investigate the entrainment and dispersibility of coal dust explosion on a laboratory scale. The rectangular cross section resembles that of an underground coal mine drift better than a circular tube. Several designs were explored to meet the requirements. The first design was a reactor entirely made of quartz glass. Figure 34 shows the design drawings.

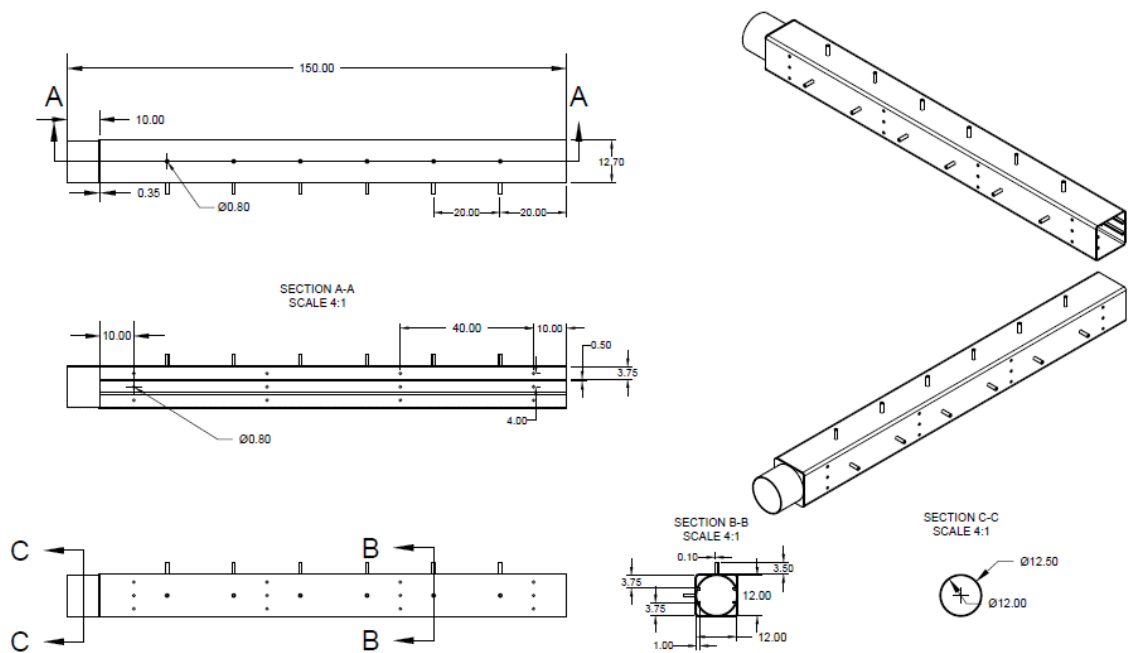


Figure 34: Quartz reactor with a length of 150 cm

The length of the reactor is 150 cm, and the cross-section is 161 cm<sup>2</sup>. The reactor contains 12 ports for ion and pressure sensors. Another element of the reactor is a measurement device located in one vertical plane along with the height of the tube equipped with three lasers to capture the dispersed coal dust concentration at different zones. One end of the quartz reactor is supposed to be connected to the existing cylindrical quartz tube (D = 12.5 cm) at CSM. On the other end of the tube, a Plexiglas containment captures the coal dust for further combustion analysis of the dust particles. Due to the complexity of the design and the fact that the reactor is made from quartz glass, the production cost exceeded the budget.

An alternative design was built from aluminum and Plexiglas. As shown in Figure 35 the sidewalls consist of plexiglass for an insight view into the reactor. Two U-channels are used on the bottom and top for stabilization. Plexiglas side walls are sealed against the metal channel with a graphite gasket.



**Figure 35: Experimental reactor with a length of 153 cm**

Additional silicon is used to seal it completely. At the one end, the reactor is covered with a 12.7 mm thick layer of plexiglass with an opening to slide in the steel tube. The other end of the reactor is open. For safety reasons, the combustible mixture will only be ignited in the steel reactor. The design ensures no backflow of ambient air and an even flow throughout the reactor. The plexiglass segments are bolted to the aluminum channels and are easy to change in the case of damage. This design also assures a complete observation to examine the evolution of the coal dust propagation over the whole length of the reactor. High-speed imaging and schlieren imaging will provide insight into the entrainment and burning coal particles as the methane flame passes through the zone containing the coal dust particles. The measuring systems are ion sensors to record the development of the flame velocity and pressure transducer, which detect the pressure wave. In total, six sensor ports are located at the top of the reactor at 25 cm distance intervals. The dimensions of the reactor are designed to use any cylindrical shaped reactor, which was designed from researchers at CSM.

---

## 5 Conclusions and recommendations for future work

---

Experiments with coal dust and a methane-air mixture in a steel tube ( $L = 153$  cm,  $D = 6.3$  cm) and the planning and construction of a reactor for a visual representation of flame propagation were the tasks of this master thesis. The aim was to compare methane-air mixture explosions to coal dust – methane – air explosions in scaled laboratory experiments. This was done by measuring flame velocity using ion sensors. The coal dust experiments were carried out with different fuel concentrations and compared coal dust deposited on a board with pre-dispersed coal dust. The highest flame propagation velocity was achieved with the reactor containing only a horizontal metal plate. The average flame speed decreased with the amount of coal dust added. This effect was observed both with deposited and with pre-injected pulverized coal. It appears that the pulverized coal in the reactor causes radiative absorption of the energy because the residence time in the steel reactor is too short. The coarse coal dust particles cool the flame temperature, as the initial energy of the explosion is too low to cook off volatile carbohydrates from the coal particles. Therefore, only the finest particles take part in the reaction. A second effect of adding coal dust as fuel reduces the available oxygen and renders the methane-air-coal dust mixture lean.

Suggestions for future research work for a better understanding of coal dust explosions:

1. Due to the comparatively low  $L/D$  ratio, it may not be possible to demonstrate flame propagation effects of the coal dust. However, other researchers were successful using coal dust in 20-liter vessels that have a diameter of  $\sim 0.3$  m. Additional investigations should be carried out in which the  $L/D$  ratio is increased, which can lead to higher energy output.
2. Additional experiments where the coal dust is placed further from the closed end. In this experiment, the coal dust was placed 20 cm downwind from the spark. In this area, flame speed may have been too low to get full mixing of the dust.

3. Coal dust explosions with different methane concentrations, especially for the lower explosion limit of methane, as this is a critical value in underground coal mines.
4. Experiments with the rectangular reactor to investigate the entrainment and dynamic dust turbulence of carbon particles.
5. Recording coal dust explosions with streak photography in a quartz glass reactor for a more detailed study of the thermal convection of the combustion of the particles.
6. CFD numerical modeling of these explosion tests.

---

## 6 References

---

- Ajrash, Mohammed J., Zanganeh, J., & Moghtaderi, B. (2017a). Deflagration of premixed methane–air in a large scale detonation tube. *Process Safety and Environmental Protection*, 109, 374–386. <https://doi.org/10.1016/j.psep.2017.03.035>
- Ajrash, Mohammed J., Zanganeh, J., & Moghtaderi, B. (2017b). Impact of suspended coal dusts on methane deflagration properties in a large-scale straight duct. *Journal of Hazardous Materials*, 338, 334–342. <https://doi.org/10.1016/j.jhazmat.2017.05.030>
- Ajrash, Mohammed Jabbar, Zanganeh, J., & Moghtaderi, B. (2016). Methane-coal dust hybrid fuel explosion properties in a large scale cylindrical explosion chamber. *Journal of Loss Prevention in the Process Industries*, 40, 317–328. <https://doi.org/10.1016/j.jlp.2016.01.009>
- Ajrash, Mohammed Jabbar, Zanganeh, J., & Moghtaderi, B. (2017). The effects of coal dust concentrations and particle sizes on the minimum auto-ignition temperature of a coal dust cloud. *Fire and Materials*, 41(7), 908–915. <https://doi.org/10.1002/fam.2437>
- Amyotte, P. R., & Pegg, M. J. (1993). Explosion hazards in underground coal mines. *Toxicological & Environmental Chemistry*, 40(1–4), 189–199. <https://doi.org/10.1080/02772249309357943>
- Azam, S., & Mishra, D. P. (2019). Effects of particle size, dust concentration and dust-dispersion-air pressure on rock dust inertant requirement for coal dust explosion suppression in underground coal mines. In *Process Safety and Environmental Protection* (pp. 35–43). <https://doi.org/10.1016/j.psep.2019.03.030>
- Barone, T. L., Patts, J. R., Janisko, S. J., Colinet, J. F., Patts, L. D., Beck, T. W., & Mischler, S. E. (2017). Sampling and analysis method for measuring airborne coal dust mass in mixtures with limestone (rock) dust. *Physiology & Behavior*, 176(1), 139–148. <https://doi.org/10.1016/j.physbeh.2017.03.040>
- Brune, J. F., Cashdollar, K. L., & Zipf, R. K. (2007). *Explosion Prevention in US Mines*. 2007, p.7. <http://www.cdc.gov/niosh/mining/UserFiles/works/pdfs/epius.pdf>
- Brune, J. F., & Goertz, B. (2013). *Lessons Learned from Mine Disasters: New Technologies and Guidelines to Prevent Mine Disasters and Improve Safety*. 1, 1–101.
- Cao, W., Gao, W., Liang, J., Xu, S., & Pan, F. (2014). Flame-propagation behavior and a dynamic model for the thermal-radiation effects in coal-dust explosions. *Journal of Loss Prevention in the Process Industries*, 29(1), 65–71. <https://doi.org/10.1016/j.jlp.2014.02.002>
- Cashdollar, K. L. (1996). *Overview of dust explosibility characters* (p. 17). <https://www.cdc.gov/niosh/mining/UserFiles/works/pdfs/odec.pdf>
- Cashdollar, K.L., Zlochower, I. A., Green, G. M., Thomas, R. A., & Hertzberg, M. (1996). *Flammability of methane, propane, and hydrogen gases*.

- Cashdollar, Kenneth L. (1996). Coal dust explosibility. *Journal of Loss Prevention in the Process Industries*, 9(1 SPEC. ISS.), 65–76. [https://doi.org/10.1016/0950-4230\(95\)00050-X](https://doi.org/10.1016/0950-4230(95)00050-X)
- Cashdollar, Kenneth L., & Hertzberg, M. (1985). *20-l explosibility test chamber for dusts and gases*.
- Cashdollar, Kenneth L., & Sapko, M. J. (2006). Explosion hazards of coal dust in the presence of methane. In *Handbook for methane control in mining*. <https://doi.org/10.1006/jfan.1995.1087>
- Christakis, N., Wang, J., Patel, M. K., Bradley, M. S. A., Leaper, M. C., & Cross, M. (2006). Aggregation and caking processes of granular materials: Continuum model and numerical simulation with application to sugar. *Advanced Powder Technology*, 17(5), 543–565. <https://doi.org/10.1163/156855206778440480>
- Cybulski, W. (1975). Coal dust explosions and their suppression. *Polish Book Translation*.
- Dastidar, A. G., Amyotte, P. R., & Pegg, M. J. (1997). Factors influencing the suppression of coal dust explosions. *Fuel*, 76(7), 663–670. [https://doi.org/10.1016/S0016-2361\(97\)00039-2](https://doi.org/10.1016/S0016-2361(97)00039-2)
- Du Plessis, J. J. L. (2015). Active explosion barrier performance against methane and coal dust explosions. *International Journal of Coal Science & Technology*, 2(4), 261–268. <https://doi.org/10.1007/s40789-015-0097-7>
- Du Plessis, J. J., & Saleh, J. (2017). *Coal Mine Explosions and the Development of Mitigating Controls*.
- Eades, R. (2016). *Modern Rock Dust Development and Evaluation for Use in Underground Coal Mines*. 110. <https://doi.org/10.13023/ETD.2016.034>
- Eades, R., Perry, K., Johnson, C., & Miller, J. (2018). Evaluation of the 20 L dust explosibility testing chamber and comparison to a modified 38 L vessel for underground coal. In *International Journal of Mining Science and Technology* (Vol. 28, Issue 6, pp. 885–890). <https://doi.org/10.1016/j.ijmst.2018.05.016>
- Fig, M. (2019). *The Impact of Environmental Conditions on Methane-Air Explosion Development and Propagation Through Rock Rubble in Confined Spaces*.
- Fleming, J. R., & Koster, J. W. (1917). *The use of permissible explosives in the coal mines of Illinois, Issues 139-143*.
- Gildfind, D. E., & Morgan, R. G. (2014). A new shock tube configuration for studying dust-lifting during the initiation of a coal dust explosion. *Journal of Loss Prevention in the Process Industries*, 29(1), 198–208. <https://doi.org/10.1016/j.jlp.2014.02.011>
- Goertz, B. (2017). *Recommendation for the prevention and suppression of coal dust explosions underground*.
- Goertz, B., Brune, J. F., Wood, C. a, & No, G. (2013). *Identifying Improved Control Practices and Regulations to Prevent Methane and Coal Dust Explosions in the United States. 1*.
- Harris, M., Cashdollar, K., Man, C., & Thimons, E. (2009). Mitigating Coal Dust Explosions in Modern Underground Coal Mines. *SSRN Electronic Journal*, 1. <https://doi.org/10.2139/ssrn.3035297>

- Harris, M. L., Sapko, M. J., Zlochower, I. A., Perera, I. E., & Weiss, E. S. (2015). Particle size and surface area effects on explosibility using a 20-L chamber. *Journal of Loss Prevention in the Process Industries*, 37, 33–38. <https://doi.org/10.1016/j.jlp.2015.06.009>
- Health, T. N. I. for O. S. and. (2011). *Mining Feature: Coal Mine Explosion Prevention*.
- Hertzberg, M., Cashdollar, K. L., & Opfermann, J. . (1979). *The flammability of coal dust-air mixtures. Lean limits, flame temperatures, ignition energies, and particulate size effects. Report of investigations*.
- Huang, Q., Honaker, R., Perry, K., & Lusk, B. (2015). Oleate-modified rock dust for wet applications in underground coal mines. *Transactions of Society for Mining, Metallurgy and Exploration*, 338(1), 448–456.
- Kalejaiye, O., Amyotte, P. R., Pegg, M. J., & Cashdollar, K. L. (2010). Effectiveness of dust dispersion in the 20-L Siwek chamber. *Journal of Loss Prevention in the Process Industries*, 23(1), 46–59. <https://doi.org/10.1016/j.jlp.2009.05.008>
- Kissel, F. N. (2006). Facts about methane that are important to mine safety. In *Handbook for methane control in mining*.
- Klemens, R., Szatan, B., Gieras, M., Wolanski, P., Maranda, A., Nowaczewski, J., & Paszula, J. (2000). Suppression of dust explosions by means of different explosive charges. *Journal of Loss Prevention in the Process Industries*, 13, 265–275. [https://doi.org/10.1016/S0950-4230\(99\)00050-9](https://doi.org/10.1016/S0950-4230(99)00050-9)
- Kundu, S., Zanganeh, J., & Moghtaderi, B. (2016). A review on understanding explosions from methane-air mixture. *Journal of Loss Prevention in the Process Industries*, 40, 507–523. <https://doi.org/10.1016/j.jlp.2016.02.004>
- Lacey, M. J. (1921). *Dust explosions and their prevention*. 26 p. [2 leaves of plates folded in side the back.
- Liao, Q., Feng, G., Fan, Y., Hu, S., Shao, H., & Huang, Y. (2018). Experimental investigations and field applications of chemical suppressants for dust control in coal mines. *Advances in Materials Science and Engineering*, 2018. <https://doi.org/10.1155/2018/6487459>
- Liu, Q., Bai, C., Li, X., Jiang, L., & Dai, W. (2010). Coal dust/air explosions in a large-scale tube. *Fuel*, 89(2), 329–335. <https://doi.org/10.1016/j.fuel.2009.07.010>
- Luo, Y., Wang, D., & Cheng, J. (2017). Effects of rock dusting in preventing and reducing intensity of coal mine explosions. *International Journal of Coal Science & Technology*, 4(2), 102–109. <https://doi.org/10.1007/s40789-017-0168-z>
- Man, C. K., Harris, M. L., & Weiss, E. S. (2010). *Determining Flame Travel Measurements from Experimental Coal Dust Explosions*.
- Medic-Pejic, L., García Torrent, J., Fernández-Añez, N., & Lebecki, K. (2015). Experimental study for the application of water barriers to Spanish small cross section galleries. *Dyna*, 82(189), 142–148. <https://doi.org/10.15446/dyna.v82n189.42689>
- Merrick, D. (1983). Mathematical models of the thermal decomposition of coal. 1. The evolution of volatile matter. *Fuel*, 62(5), 534–539.

[https://doi.org/10.1016/0016-2361\(83\)90222-3](https://doi.org/10.1016/0016-2361(83)90222-3)

- Michelis, J. (1996). *Entwicklung und Untersuchung eines betrieblichen anwendbaren Verfahrens zur messtechnischen Ueberwachung der Wirksamkeit von Staubbindemitteln unter Tage.*
- Michelis, J. (1998). *Explosionsschutz im Bergbau unter Tage.*
- Mishra, D. P., & Azam, S. (2018). Experimental investigation on effects of particle size, dust concentration and dust-dispersion-air pressure on minimum ignition temperature and combustion process of coal dust clouds in a G-G furnace. In *Fuel* (Vol. 227, pp. 424–433). <https://doi.org/10.1016/j.fuel.2018.04.122>
- MSHA. (2003). *Internal Review of MSHA's Actions at the No. 5 Mine Jim Walter Resources, Inc. Brookwood, Tuscaloosa County, Alabama. 5.*
- MSHA. (2012). *Internal Review of MSHA's Actions at the Upper Big Branch Mine-South Performance Coal Company Montcoal, Raleigh County, West Virginia.*
- Nagy, J. (1981). The explosion hazard in mining. In *U.S. Department of Labor Mine Safety and Health Administration.*
- Nagy, J., & Verakis, H. C. (1983). *Development and control of dust explosions.*
- Nagy, John., Kawenski, E. M., & Mitchell, D. W. (1965). *Float coal hazard in mines: a progress report* (p. 15 p.). U.S. Dept. of the Interior, Bureau of Mines. <file://catalog.hathitrust.org/Record/005982068>
- National Academies of Sciences, Engineering, and M. (2018). *Monitoring and Sampling Approaches to Assess Underground Coal Mine Dust Exposures.*
- Ng, D., Sapko, M., Furno, A., & Pro, R. (1987). Coal Dust and Gas Explosion Suppression by Barriers. In *Industrial Dust Explosions*. ASTM International. <https://doi.org/10.1520/STP28171S>
- Page, N. G., Watkins, T. R., Caudill, S. D., Cripps, D. R., Godsey, J. F., Maggard, C. J., Moore, A. D., Morley, T. A., Phillipson, S. E., Sherer, H. E., & Steffey, D. A. (2011). Report of investigation, fatal underground mine explosion, April 5, 2010, Upper Big Branch Mine-South, Performance Coal Company, Montcoal, Raleigh County, West Virginia, ID No. 46-08436. In *United States Department of Labor Mine Safety and Health Administration Coal Mine Safety and Health Report.*
- Parr, S. W. (1911). The determination of volatile matter in coal. *Industrial and Engineering Chemistry*, 3(12), 900–902. <https://doi.org/10.1021/ie50036a005>
- Perera, I. E., Sapko, M. J., Harris, M. L., Zlochower, I. A., & Weiss, E. S. (2016). Design and development of a dust dispersion chamber to quantify the dispersibility of rock dust. *Journal of Loss Prevention in the Process Industries*, 39, 7–16. <https://doi.org/10.1016/j.jlp.2015.11.002>
- Roychowdhury, S. N. (1960). *Coal dust explosion and their prevention*. Missouri University of Science and Technology.
- Sapko, M. J., Cashdollar, K. L., & Green, G. M. (2007). Coal dust particle size survey of US mine. *Journal of Loss Prevention in the Process Industries*, 20(4–6), 616–620. <https://doi.org/10.1016/j.jlp.2007.04.014>
- Sapko, M. J., Weiss, E. S., & Cashdollar, K. L. (2006). Float Coal Dust Explosion

- Hazards. *Technology News: DHHS (NIOSH) Publication No. 2006–125*, 4(515), 2.
- Sapko, M. J., Weiss, E. S., Cashdollar, K. L., & Zlochower, I. A. (1996). *Experimental mine and laboratory dust explosion research at NIOSH*. October.
- Schafner, J. R. (2018). *Management of coal dust explosions in United States' coal mines using bag type passive explosion barriers*. [https://scholarsmine.mst.edu/masters\\_theses/7782](https://scholarsmine.mst.edu/masters_theses/7782)
- Si, R., Li, R., & Huang, Z. (2012). Material evidence analysis upon accident investigation of gas and coal dust explosion. *Procedia Engineering*, 45, 458–463. <https://doi.org/10.1016/j.proeng.2012.08.186>
- Stephan, C. R. (1998). *Coal Dust Explosion Hazard*.
- Strebinger, C. (2019). *Modeling large-scale high-speed methane gas deflagrations in confined space: Applications for longwall coal mines*.
- Torrent, J. G., & Fuchs, J. C. (1989). *Flammability and explosion propagation of methane/coal dust hybrid mixtures*.
- Zipf, R. K., Gamezo, V. N., Sapko, M. J., Marchewka, W. P., Mohamed, K. M., Oran, E. S., Kessler, D. A., Weiss, E. S., Addis, J. D., Karnack, F. A., & Sellers, D. D. (2013). Methane-air detonation experiments at NIOSH Lake Lynn Laboratory. *Journal of Loss Prevention in the Process Industries*, 26(2), 295–301. <https://doi.org/10.1016/j.jlp.2011.05.003>
- Zou, D. H., & Panawalage, S. (2001). *Passive and Triggered Explosion Barriers in Underground Coal Mines - A literature review of recent research*.

---

## 7 List of figures

---

Figure 1: Flammable limits of a methane-air-coal mixture (Cashdollar & Sapko, 2006).....	7
Figure 2: Schematic of different explosion preventions and the methods and applications behind it.....	16
Figure 3: Design of the polish stone dust barrier.....	18
Figure 4: Statistic of coal mine explosion fatalities from the 1900s (National Academies of Sciences, Engineering, and Medicine 2018).....	21
Figure 5: Schematic drawing of the experimental set-up of Chinese reactor: 1) experimental tube, 2) dispersion system, 3) ignition system, 4) DAQ system, 5) pressure sensor, 6) control unit, 7) vacuum pump, 8) venting system, 9) air pump, 10) connecting system, 11) plastic membrane, and 12) silencer(Liu et al., 2010)	27
Figure 6: Schematic drawing of the experimental set-up of Australian reactor (Ajrash et al., 2017a).....	28
Figure 7: Experimental setup of the reactor in Kloppersbos, South Africa. Left: aerial view, right: view of the open end.....	29
Figure 8: Schematic diagram of the reactor with the length of methane, coal dust and rock dust zones (Du Plessis, 2015).....	29
Figure 9: Experimental setup of reactors at CSM. Left: Quartz reactor for visual methane explosion and steel reactor; Right: View of the large-scale reactor at the Edgar Mine (Fig, 2019; Strebinger, 2019).....	30
Figure 10: Schematic layout of the experimental steel reactor with all components in the laboratory at CSM.....	31
Figure 11: Left: The 6.3 cm diameter and 153 cm long steel reactor inserted in the 30.5 cm diameter steel reactor with a black hose from the top for the exhaust and the box with the DAQ for the ion sensors; Right: View to the open-end of the steel reactor with high speed imaging and the exhaust box at the open end of the T-junction.....	34
Figure 12 Left: Schematic of the ion sensor circuit. Value of voltage source is 54 V, value of resistor is 1 M $\Omega$ , Right: Metal box with the DAQ system, the four voltage sources for the four sensors and the connection to the DAQ.....	34
Figure 13: Typical signal from passing of the flame. In this case the flame was produced by a torch. Each color represents an ion sensor and the first rise, described as flame detection (FD), of each line correspond to the first detection of the flame in voltage as a function of time.....	35

Figure 14: Signal from passing the flame of a lighter. The voltage peaks are weaker than the peaks from Figure 14.....	36
Figure 15: Deposited coal dust on the metal plate .....	36
Figure 16: Schematic of the spark ignition system (Strebinger, 2019) .....	38
Figure 17: Output from the ion sensors with Scout. X-axis is a function of the Index which refers to the numbers of samples taken with a specific sample rate (Hz)...	40
Figure 18: Impact of stoichiometric mixture on methane flame front propagation velocity; mixture volume is within $\pm 0.3$ %; $SD_{\text{mean}} = 26\%$ .....	41
Figure 19: Image of a stoichiometric flame leaving the open-end of the steel reactor .....	41
Figure 20: Impact of stoichiometric mixture on methane flame front propagation velocity; mixture volume is within $\pm 0.3$ %; $SD_{\text{mean}} = 7.9$ % .....	42
Figure 21: Impact of stoichiometric mixture on flame front propagation velocity; mixture volume is within $\pm 0.3$ %; $SD_{\text{mean}} = 8.1$ % .....	44
Figure 22: Impact of stoichiometric mixture on flame front propagation velocity; mixture volume is within $\pm 0.3$ %; $SD_{\text{mean}} = 9.3$ % .....	45
Figure 23: Impact of stoichiometric mixture on flame front propagation velocity; mixture volume is within $\pm 0.3$ %; $SD_{\text{mean}} = 12$ % .....	46
Figure 24: Impact of stoichiometric mixture on flame front propagation velocity; mixture volume is within $\pm 0.3$ %; $SD_{\text{mean}} = 4.5$ % .....	46
Figure 25: Average flame front propagation velocity of all tests carried out with no dust and deposited coal and rock dust; Operating conditions: $294 \pm 1$ K, $83 \pm 1$ kPa and $E_{\text{ign}}=60 \pm 5$ mJ .....	48
Figure 26: Average flame front propagation velocity of all tests carried out with no coal dust and deposited coal; Operating conditions: $294 \pm 1$ K, $83 \pm 1$ kPa and $E_{\text{ign}}=60 \pm 5$ mJ .....	49
Figure 27: Modified schematic layout of the experimental steel reactor with all components to pre-disperse the coal dust into the reactor. The red circle indicates the line and valve to inject the dust .....	50
Figure 28: Impact of stoichiometric mixture on flame front propagation velocity; mixture volume is within $\pm 0.3$ %; $SD_{\text{mean}} = 13.9$ % .....	51
Figure 29: Impact of stoichiometric mixture on flame front propagation velocity; mixture volume is within $\pm 0.3$ %; $SD_{\text{mean}} = 9.0$ % .....	52
Figure 30: Impact of stoichiometric mixture on flame front propagation velocity; mixture volume is within $\pm 0.3$ %; $SD_{\text{mean}} = 14.4$ % .....	53

Figure 31: Impact of stoichiometric mixture on flame front propagation velocity; mixture volume is within  $\pm 0.3\%$ ;  $SD_{mean} = 8.1\%$  ..... 53

Figure 32: Comparison of the mean flame front propagation velocity for test with the metal plate in the steel reactor ..... 54

Figure 33: Images of the experiment with 0.5 g of pre-dispersed coal dust before ignition. Flame was filmed from the side of the open end of the steel reactor. .... 55

Figure 34: Quartz reactor with a length of 150 cm..... 56

Figure 35: Experimental reactor with a length of 153 cm ..... 57

---

## 8 List of tables

---

Table 1: Specification of the Pittsburgh coal dust.....	37
Table 2: Summary of all experiments carried out and the mean flame front propagation velocities ( $\bar{v}$ ) and mean standard deviations ( $\overline{SD}$ ) of each series of test .....	39
Table 3: Overview of conducted test in steel reactor with metal plate and dust ...	44
Table 4: Overview of all tests carried with the metal plate inside the reactor. ....	47

---

## 9 List of abbreviation

---

USBM	United States Bureau of Mines
NIOSH	The National Institute for Occupational Safety and Health
MSHA	Mine Safety and Health Administration
LLEM	Lake Lynn Experimental Laboratory
UBB	Upper Big Branch Mine
BEM	Bruceston Experimental Mine
LEL	Lower Explosive Limit
UEL	Upper Explosive Limit
MFC	Mass Flow Controller
MFM	Mass Flow Meter
CO	Colorado
DAQ	Data Acquisition
L/D ratio	Length to Diameter ratio
CFR	Code of Federal Regulations
SLPM	Standard Liter per Minute
$\bar{V}_{x-y}$	Mean flame front propagation velocity between two known points
$\bar{SD}_{x-y}$	Mean standard deviation of flame front propagation velocity between two known points
CFD	Computational Fluid Dynamics

---

# Appendices

---

## Appendix A:

### Operation of the Steel Flame Reactor

---

#### 1. Pre-Filling

---

- 1.1. Verify building exhaust is properly functioning
  - 1.2. Visually inspect gas lines and fittings for loose connections or mechanical damage
  - 1.3. Verify that gas leak detector is in place and functioning
  - 1.4. Verify spark system is working properly
  - 1.5. Open valve to building air supply
  - 1.6. Check to ensure ion sensors are working properly by collecting data and touching each sensor
  - 1.7. Ensure gas supply mass flow controllers are functioning properly
  - 1.8. Ensure aluminum foil covering is fitted on the open end
  - 1.9. Ensure exhaust on the open end of T-junction of the steel tube is in place and that pressure relief valve is exhausted properly
- 

#### 2. Filling of the Steel Tube

---

- 2.1. Switch the "**Premix valve**" (manually) to **OPEN** and "**Purge valve**" to **CLOSE**. Both valves are next to the steel tube
- 2.2. Flip Control Panel Switch to "**Methane Off**," "**Building Air**" and "**Fill**"
- 2.3. Building air flows through the system into the reactor now
- 2.4. Check for any leaks in gas lines and fittings
- 2.5. The open valve of compressed air tank and methane gas tank
- 2.6. Begin flowing the compressed air by the flipping switch on the control panel to "**Air On**"
- 2.7. Regulate the Airflow rate by adjusting the valve next to the Air MFC
- 2.8. Switch the "**Gas-Purge valve**" to **CLOSE**. This valve is also located in the gas cabinet
- 2.9. Switch the "**CH<sub>4</sub> gas valve**" manually to **OPEN**. The valve is in the gas cabinet
- 2.10. With air flowing, flip the control panel switch to "**Methane On**"
- 2.11. Begin countdown of fill timer according to flow rate.
- 2.12. **Manually CLOSE** the "**Premix valve**" and **OPEN** the "**Purge valve**" next to the steel tube
- 2.13. **CLOSE** the "**Gas valve**" and **OPEN** the "**Gas-Purge valve**" and **OPEN SLOWLY** the building air valve to purge the methane lines.
- 2.14. Wait **1 minute** for purge to complete, and gases become stagnant
- 2.15. Ignite mixture by flipping spark system switch on and off for a single spark
- 2.16. After the combustion event is complete, flip the "**Premix Valve**" to **OPEN** and "**Purge Valve**" to **CLOSE** to purge the reactor for at least **5 Minutes**.
- 2.17. Remove the rest of the coal dust from the steel tube.

---

### 3. Post-Performance

---

- 3.1. Ensure the main valve on all gas tanks is fully closed and **pressure reads zero**
- 3.2. Ensure control panel switches are on "**Methane Off**," "**Building**," and "**Purge Quartz tube**."
- 3.3. Ensure all lines and tubes have been purged
- 3.4. Building supply valves are closed
- 3.5. Ensure the spark system is disconnected and stored safely
- 3.6. Ensure ventilation system is turned off

## Appendix B:

### What-If Analysis as a safety measures in an emergency

What IF?	Answer	Recommendation
Power ist lost during filling of methane/air mixture of the tube?	Emergency power generator will turn on to provide electricity for the ventilation system	
Laboratory ventilation is lost?	Emergency power generator will turn on to provide electricity for the ventilation system	Check ventilation system before doing the tests
There is an unexpected over-pressurization in the lines?	Pressure relief valve before the mixing tank is installed to keep pressure at a safe level	Ensure line connections are properly connected and do not leak; MFCs work
Filling procedure was being done wrong?	Purge the CH <sub>4</sub> /air mixture with air to the exhaust system for a certain amount of time	Ensure line connections are properly connected and do not leak; MFCs work
MFCs stop working during fill process?	Turn off methane tank; Purge the CH <sub>4</sub> /air mixture with air to the exhaust system for a certain amount of time	Control MFCs during filling process if there are some unexpected events
The spark system does not work to ignite the mixture in the tube?	Purge the CH <sub>4</sub> /air mixture with air to the exhaust system for a certain amount of time	Ensure battery is charged and circuit of battery is connected right;
A gas/premix line is leaking?	Turn off methane tank; Purge all lines with air	Ensure prior that lines do not leak
The alarm system for dangerous methane concentration goes on?	Press the emergency stop button installed near experimental setup; open window; call EHS 303-273-3316	Ensure prior that lines do not leak
Material catches fire after the explosion?	Press the emergency stop button installed near experimental setup; Extinguish the fire with one of the 4 fire extinguisher located in the lab	Ensure all combustibile materials kept removed from contact with flame and tube opening during operation
Coal dust gets reignited after the shot?	Press the emergency stop button installed near experimental setup; Extinguish the fire with one of the 4 fire extinguisher located in the lab	Ensure all combustibile materials kept removed from contact with flame and tube opening during operation
A human is exposed to gases or smoke?	Call 911 to reach Police, Fire or Ambulance Service; provide first aid	Ensure prior that lines do not leak
Methane/air mixture does not ignite in the tube?	Purge the CH <sub>4</sub> /air mixture with air to the exhaust system for a certain amount of time	Ensure if the setting on MFC are correct; ensure that the spark system works
Reactor bursts during explosion?	Call 911 to reach Police, Fire or Ambulance Service; provide first aid	